FGF signalling plays similar roles in development and regeneration of the skeleton in the brittle star *Amphiura filiformis*

Authors:

Anna Czarkwiani[1,#,*], David V. Dylus[1,2,‡,*], Luisana Carballo[1,†], and Paola Oliveri[1,3]

Affiliations:

[1] Department of Genetics, Evolution and Environment, University College London, London, United Kingdom

[2] Centre for Mathematics, Physics and Engineering in the Life Sciences and Experimental Biology, University College London, London, United Kingdom

[3] Centre for Life's Origin and Evolution (CLOE), University College London, London, United Kingdom

[#]Author's current address: Centre for Regenerative Therapies Dresden, Dresden, Germany

[‡] Author's current address: Department Computational Biology & Centre for Integrative Genomics, University of Lausanne, Lausanne, Switzerland

[†] Author's current address: Department of Behavioural Ecology & Evolutionary Genetics, Max Planck Institute for Ornithology, Seewiesen, Germany

* These authors contributed equally to this work.

Corresponding author:

Paola Oliveri, p.oliveri@ucl.ac.uk

Key Words: Echinoderm, biomineralization, regulatory networks, signalling, VegF

Abstract

Regeneration as an adult developmental process is in many aspects similar to embryonic development. Although many studies point out similarities and differences, no large-scale, direct and functional comparative analyses between development and regeneration of a specific cell type or structure in one animal exist. Here, we use the brittle star *Amphiura filiformis* to characterise the role of the FGF signalling pathway during skeletal development in embryos and arm regeneration. In both processes, we find ligands expressed in ectodermal cells flanking underlying skeletal mesenchymal cells, which express the receptors. Perturbation of FGF signalling showed inhibited skeleton formation in both embryogenesis and regeneration, without affecting other key developmental processes. Differential transcriptome analysis finds mostly differentiation genes rather than transcription factors to be downregulated in both contexts. Moreover, comparative gene analysis allowed us to discover brittle star specific, differentiation genes. In conclusion, our results show that the FGF pathway is crucial for skeletogenesis in the brittle star, as in other deuterostomes and provide evidence for the re-deployment of a developmental gene regulatory module during regeneration.

Introduction

A tempting theory for the evolutionary origins of tissue regeneration suggests it was selected as a secondary by-product of development and thus sharing many similarities with embryogenesis (1,2). In fact, following the unique processes of regeneration (such as wound healing and dedifferentiation), cell specification and differentiation must occur just like during embryonic development. Studies showed that gene expression during development and regeneration can be conserved. For instance, in newt the sonic hedgehog gene recapitulates its role in developing limb buds during adult regeneration (3); and during elbow joint regeneration in developing chick embryos (4). *Meis* genes under control of the retinoic acid signalling pathway are also involved in salamander limb regeneration similarly to their role during embryonic limb development (5). In planarians many of the components of the genetic network underlying eye development in other species (e.g., *otx*, *six*, *opsin*) have been shown to be expressed and functionally required during adult eye regeneration, although others (i.e. *pax6)* play no role in this context, underlying some important differences (6,7). Unravelling the function of signalling pathways and transcription factors in development and regeneration can thus shed light on whether adult organisms with the capability of regeneration re-use developmental gene regulatory networks. However, few studies exist, and these mostly compare the expression of a single gene between development and regeneration in the same organism. With new transcriptomic databases (e.g. Iberian ribbed newt (8) and the sea anemone (9)) comparative analysis showed that embryonic gene regulatory networks are partially re-used during adult sea anemone whole body regeneration.

Consistent with the idea that the initiation of regeneration is very different from embryonic development, several genes have been identified that are unique to regeneration (10).

Comparing the role of signalling pathways in embryogenesis and regeneration provides a compelling strategy to understand the extent of similarities between gene regulatory networks driving these two developmental processes. A good example of this is the fibroblast growth factor (FGF) signalling pathway, implicated in a wide range of biological processes such as cell migration, differentiation and proliferation, during development, wound healing and regeneration (11,12). Regeneration in hydra, zebrafish, *Xenopus* and salamanders relies on the expression of FGF genes, and applying FGFR inhibitors results in regenerative defects (13–18). The FGF signalling pathway also plays important roles in development and regeneration of the vertebrate skeleton. Mutations in both ligands and receptors were found to cause a variety of congenital disorders including craniosyntoses, chondrodysplasia (19–21), and multiple types of gross skeletalal abnormalities in mouse models and humans (22). Similarly, multiple FGFs and FGFRs are expressed during fracture healing and bone regeneration (23). Importantly, the precise roles and effects of FGF inhibition during postembryonic morphogenesis are not well understood (24).

The role of FGF signalling in skeletogenesis also extends to echinoderms, which are an excellent experimental system for studying the gene regulatory networks (GRN) underlying development (25–28). FGF signalling is necessary for guiding skeletogenic mesenchymal cell migration and formation of the embryonic skeleton in the sea urchin *Paracentrotus*

lividus (29). Interestingly, in a different species, *Lytechinus variegatus*, FGF inhibition using *fgf9/16/20* morpholino (also called *fgfa*) produces a much milder phenotype in comparisons to *P. lividus* (29), whereby the mesenchymal cells migrate normally and the embryos form shortened skeletal rods (30). In addition to FGF, the VEGF signalling pathway is also involved in skeletogenesis in both species. Perturbation of the *vegf3* ligand in the sea urchin interferes with both correct skeletogenic cell migration and skeletal rod formation (30–32). It seems clear that both of these pathways have essential, often interconnected and non-redundant roles in skeletogenesis in the sea urchin embryo. However, whether these pathways regulate different downstream effector genes, and whether their role is conserved during adult skeletogenesis in echinoderms remain open questions.

Recently, several studies have established the brittle star *Amphiura filiformis* (*Afi*) as an experimental system for skeleton formation in both embryonic development (33,34) and adult regeneration (35,36). Characterization of these processes showed that the skeletogenic cells of both the adult and embryo are mesenchymal and express an array of skeletogenic specification transcription factors such as *alx1,* a gene that has a conserved role in skeleton development in echinoderms (37), and vertebrates (38,39). Adult skeletogenic cells also express downstream embryonic skeletal differentiation genes, including *c-lectin, p58b, p19* and *α-coll* (33,35,36). Moreover, transcriptomic data for both the embryonic stages (34,40) and the adult regenerating and non-regenerating arms (41,42) are now available. With this wealth of information on regeneration and early development of the

skeleton, this species can be used to directly compare the role of FGF signalling in both processes within the same animal at different life stages.

In this study, we carry out a large-scale, side-by-side comparison of the development of the skeleton during embryogenesis and adult regeneration in the context of FGF signalling. We first characterize the expression of FGF signalling components during morphologically comparable stages of the development of the skeleton in both processes. We then use an FGF signalling inhibitor (SU5402) in embryos and adult *A. filiformis* to determine the effect of disrupting this pathway. We find that perturbation of FGF signalling in brittle stars results in failure to form skeletal spicules in both the embryos and in the regenerating arms. Using an unbiased transcriptome approach comparing control and treated embryos, we find several brittle star specific skeletogenic genes. Moreover, many of these are affected similarly in embryos and in adult regenerating arms, suggesting a conservation of pathway components and network connections between these two processes. Ultimately, our study provides the first direct evidence for an analogous role of FGF signalling in skeletogenesis between embryonic development and adult regeneration in the same species working downstream from the specification tier of the skeletogenic GRN.

Results

Evolutionary relationships of FGF and VEGF signalling components in echinoderms

Both Fgf and Vegf signalling pathways are required in the development of the sea urchin larval skeleton (35-38). To characterize signalling genes in these two pathways in the brittle star *Amphiura filiformis* (*Afi*), we first

surveyed an embryonic transcriptome encompassing the entirety of development (from cleavage stage to pluteus larvae) (34), and transcriptomes from adult regenerating and non-regenerating arms (41) of *A. filiformis* for potential homologs. To do this, we combined a BLAST search using selected candidates (e-value 1e-6) from the sea urchin database (43) with a hidden Markov model search against PFAM domains of Fgf and Vegf ligands and receptors (44). Using this strategy, we found two potential Fgf ligands, three Fgf receptors, two Vegf ligands and one Vegf receptor in *A. filiformis* (Table S1).

To better understand the evolutionary relationships of our *A. filiformis* genes relative to echinoderm and chordate signalling systems, we used a collection of sequences of Fgf and Vegf ligands and receptors for 41 species spanning all major clades of echinoderms, chordates (e.g. mouse, rat etc.) and non-deuterostome outgroup species such as the pacific oyster (*Crassostrea gigas*). For each of the four datasets we computed the orthologous relationships using the Orthologous Matrix Algorithm (OMA)(45) and extracted 5 groups containing our genes (see methods for details). For each of these groups we then computed maximum likelihood phylogenetic trees using amino acid sequences. We observe that two Fgf ligands are placed in an echinoderm group sharing a common ancestor with their respectively independently duplicated genes in chordates (Fig. S1 and S2). The evolutionary relationship with the well-studied sea urchin orthologous sequences is well supported. For instance, *Afi-Fgf9/16/20* shares a highly supported common ancestor with the *Spu-Fgf9/16/20* gene (Fig S1), while the relation with chordates and hemichordates has low support values, despite

the OMA run identifying a clear gene group with the vertebrates FGF9, FGF16 and FGF20. Similar result is obtained for the ligand gene *Afi-Fgf8/17/18* with a better support to the chordate genes (Fig S2).

Different evolutionary relationships are revealed for the Fgf receptors. Three *A. filiformis* sequences are identified in the FGFR OMA group, which includes chordates FGF receptors. Afi-Fgfr1 to Afi-Fgfr2 and Afi-Tk9 are all in a group with other echinoderm FGF receptors, which include the sea urchin Sp-Fgfr (also known as Fgfr1 (46)), Sp-Fgfr2 (also known as Fn3_Ig_29 (46)) and the Sp-Tk9 respectively. All echinoderm FGF receptors have a weak relation to the group of chordate FGFR1, FGFR2 and FGFR4 receptors (Fig. S3). Our analysis suggests an evolutionary scenario in which both chordates and echinoderms independently duplicated these genes from a single common ancestor. FGF receptors are membrane proteins, with an extracellular domain consisting of three immunoglobulin-like subdomains (Ig), a trans-membrane (TM) domain, and an intracellular region encompassing a tyrosine kinase domain (PTK) (Fig. S3)(47). A protein conserved domain analysis conducted on the three potential *A. filiformis* FGF receptors shows that only Afi-Fgfr1 and Afi-Fgfr2 are equipped with all the structural domains to work as FGF receptors, while TK9 is not. Therefore, only two FGF receptors are identified in *A. filiformis* consistent to what already was reported in other echinoderms (46,48). Concerning the Vegf ligands, we also observe independent duplication events in chordates (VEGFA and VEGFB) as well as echinoderms (Vegf2 and Vegf3) (Fig. S4). Both *A. filiformis* Vegf ligands share a highly supported common ancestor with their annotated genes in sea urchin. The only VEGF receptor of echinoderms forms a sister group to three

VEGF receptor genes in chordates (Fig. S5). Here, however, we specifically focus on genes with clear orthology between the sea urchin and brittle star, as the sea urchin has a well-annotated genome. Ultimately, this analysis highlights the difficulties of drawing clear orthology among distantly related species when clade specific gene duplication and losses occurred, but importantly allows us to bring our results into a broader evolutionary context when comparing across different species.

FGF signalling genes are expressed during both embryonic development and adult arm regeneration

To better understand the role of *fgf* signalling genes in the context of britte star skeletogenesis, we first analysed the expression of ligands and receptors during embryogenesis and adult regeneration using *in situ* hybridization (ISH) and NanoString transcript quantification. For this purpose, we selected the most likely corresponding stages between development and regeneration using the established staging system for regenerating arms (49) and the developmental timeline for embryos (33) (Fig. S6A, B); and gene activity (Fig. S7A). Specifically, we focused on developmental stages when the skeletogenic lineage is segregated from other mesodermal cells and specific skeletogenic genes are expressed (blastula and mesenchyme blastula stages Fig. 1A; Fig. S6A; stage 3 during arm regeneration Fig. 1B; Fig. S6B) and when skeletal spicules appear (gastrula stage; Fig. 1A; Fig. S6A; stage 3-5 during adult arm regeneration; Fig. 1B; Fig. S6B) (33–36).

In the embryo, the *Afi-fgf9/16/20* ligand is first detectable at mesenchyme blastula stage, between 15 and 18 hours post fertilization (hpf) ubiquitously (Fig. 1A; Fig. S7A). It then becomes confined to a band in the ectodermal domain at the boundary of the endoderm, with higher expression in two domains adjacent to the clusters of mesenchymal cells that will produce the skeleton of the embryo at gastrula stage (Fig. 1A; Fig. S7A). After arm amputation there is a subtle global upregulation of *Afi-fgf9/16/20* at 48 hours post amputation (hpa) followed by a constant level of expression detectable using NanoString (Fig. S7). WMISH reveal that *Afi-fgf9/16/20* is expressed in the epidermis throughout early regenerative stages (stage 3-5; Fig. 1B). At stage 4 an additional domain adjacent to the radial water canal (RWC) became visible, within the domain of the coelomic epithelium (Ce). This expression is visible in patches of cells in the most proximal part of the Stage 5 in correspondence to where the newly forming metameric units appear in the regenerating arm (Fig. 1B). During development, the receptor *Afi-fgfr1* is expressed in the vegetal half of the embryo at blastula stage, and endoderm and non-skeletogenic mesoderm from mesenchyme blastula stage to gastrula stage (Fig. 1A; Fig. S7A). Upon amputation and after an initial drop in level of expression at 24 hpa, *Afi-fgfr1* levels increases around stage 3 of regeneration (Fig. S7A) and exhibits a highly dynamic pattern during adult arm regeneration in several territories including the epidermis, radial nerve cord, coelomic epithelium and radial water canal (Fig. 2B; Fig. S6E). Conversely, the receptor *Afi-fgfr2* is first specifically expressed in the skeletogenic mesoderm (SM) cells at mesenchyme blastula stage and

expands to the non-skeletogenic mesoderm at gastrula stage during embryonic development (Fig. 1A; Fig. S7A). During stages 4 and 5 of regeneration it is expressed in the dermal layer where the skeleton first appears during regeneration (29; Fig. 1B; Fig S6B.). Notably, global expression of *Afi-fgfr2* is relatively low in the NanoString data, which most likely reflects its specific expression only in the small population of skeletogenic cells relative to the whole arm structure (Fig S7A). Expression of FGF signalling pathway components at late stages of regeneration persist in similar territories (epidermis for the *fgf9/16/20* ligand and skeletal domains for *fgfr2* receptor; Fig. S8). Other identified components of the FGF signalling (*afi-fgf8/17/18* and *afi-tk9*) are not expressed either in cell types or at developmental/regenerative time points relevant to this study (Figure S7). Interestingly, the expression of *fgf9/16/20* in the ectoderm and the *fgfr2* receptor in mesenchymal cells is comparable to the expression of their orthologs in sea urchin development (29). With respect to the organization of mesenchymal cells and their proximity to the ligand-expressing ectodermal domain cells, sea urchin and brittle star embryos share a similar topology.

FGF signalling perturbation with SU5402 inhibits skeleton formation in both embryos and adult regenerating arms

To analyse the role of FGF signalling in skeletogenesis during brittle star embryonic development and adult arm regeneration we applied the SU5402 inhibitor, a small molecule well-known to specifically inhibit the function of FGFRs by competing with ATP for the binding site of the catalytic domain of tyrosine kinase (50). This inhibitor has been successfully used to

disrupt FGF signalling during both embryogenesis and regeneration (15, 51–53) in many organisms.

For developmental characterization, we treated brittle star embryos with SU5402, alongside non-treated filtered seawater (FSW) and DMSO (used as the solvent for the drug) controls at 18hpf (hours post-fertilization) preceding SM ingression (33). After an initial test at three different concentrations (5µM, 10µM and 20µM), 10µM of SU5402 was chosen as the optimal dilution to elicit a consistent and reproducible phenotype without arresting development. The 18hpf time point was used to avoid interfering with potential early functions of FGF signalling during cleavage stages and to specifically focus on skeletogenesis (as this also corresponds to the temporal onset of *fgfr2* expression in skeletogenic cells, see Fig. 1A and Fig. S7A). At 27hpf we collected the embryos for RNAseq and NanoString analysis (Fig. 2A) to assess the early response to signalling inhibition and to avoid secondary effects of FGF perturbation for a prolonged period. At this stage treated embryos are indistinguishable from controls showing a timely ingression of the primary mesenchymal cells. Subsequently, we scored several embryos at late gastrula and pluteus stages for the formation of spicules. All SU5402-treated embryos failed to develop skeletal spicules (100%, n=114), compared to 0.2% DMSO (13.8%, n=94) and FSW controls (26.7%, n=101) (Fig. 2B). Despite having no visible defects in SM ingression, archenteron invagination or overall survival (58 hpf; Fig. 2B), the perturbed embryos did not develop a skeleton, even at late stages of development (4 dpf; Fig. 2B).

A similar treatment was performed in regenerating arms to functionally assess the role of FGF signalling during adult skeleton regeneration. We applied the SU5402 inhibitor to amputated arm explants, which can survive separated from the main body for several weeks and continue to regenerate properly (54). The explants were incubated in 10µM SU5402 from stage 2 (prior to formation of skeletal spicules and the onset of *fgfr2* in dermal cells; (36)) for 24h after which they were scored for phenotype and collected for further analyses (Fig. 3A). FGF signalling perturbation using this method caused inhibition of skeletal spicule formation in the majority of arms (78.1%, n=41), as shown by the absence of calcein staining in the dermal layer, compared with 0.1% DMSO controls (7.7%, n=39) and non-treated FSW controls (8.1%, n=37) (Fig. 3B). All arm explants were alive and mobile after treatment (Movie S1), however only the DMSO and FSW controls continued to regenerate 48h after treatment (Fig. 4A). Since treated explants did not elongate, and to rule out possible toxic side effects, we examined whether the explants retained cell proliferation ability. Interestingly, even though SU5402 treated explants failed to regenerate further (n=8; Fig. 4A) we found that cell proliferation was not affected by the inhibition of FGF signalling (n=4; Fig. 4B,C). This provided evidence that not all cellular mechanisms have been affected by the treatment, but rather a specific effect has been exerted on regeneration of different tissues, including the skeleton. Importantly, the application of SU5402 led to a reduction of skeleton during both development and regeneration.

VEGF signalling perturbation with Axitinib mildly inhibits skeleton formation in both embryos and adult regenerating arms of A. filiformis

The VEGF signalling pathway plays a pivotal role in sea urchin skeletogenesis and the expression of its ligand in the ectoderm and of its receptor in the mesenchymal cells resembles the expression of components of the FGF pathway (56). SU5402 has been shown to have some mild inhibitory effects on this pathway at high concentrations: 50μM and above (57), therefore to determine to what extent inhibition of the VEGF pathway alone could interfere with skeletogenesis, we characterized the expression of its components (Fig. S7B and S9A,B) and inhibited it with a VEGF specific inhibitor: Axitinib, which selectively inhibits VEGF receptors by blocking their cellular autophosphorylation (58) (Fig. S9C,D). Embryos were initially incubated with different concentrations (50nM, 75nM and 100nM) of inhibitor to determine the optimal condition (75nM) to induce reproducible phenotype without arresting development. Interestingly, although the expression patterns of VEGF ligands and receptors is strikingly similar to FGF components in embryos and regenerates in the brittle star (Fig. S9A,B), inhibition of the VEGF signalling pathway using Axitinib resulted in a much milder phenotype in respect to skeleton development in the embryos and regenerating explants of *A. filiformis* compared with the phenotype obtained with SU5402 treatment (compare Fig. 2 and 3 with Fig. S9C,D). Axitinib-treated embryos usually formed one spicule during early development and this spicule elongated but failed to be patterned correctly (n=89/118) compared with normal skeletogenesis in FSW (n=102/119) and DMSO controls (n=101/123) (Fig. S9C). Only 36.6% of treated explants (n=41) showed reduced or absent

spicules compared to 13.6% in DMSO controls (n=44) and 10% in FSW controls (n=40) (Fig. S9D). At the concentration used in this study, it is unlikely that SU5402 inhibition impinges significantly on the VEGF pathway, and specific inhibition of VEGF signalling shows that it is not strictly required for biomineralization to occur, but most likely for further patterning of the skeletal elements. We thus only focused on the molecular network affected by SU5402 treatment from this point on.

Many genes downregulated by SU5402 are expressed specifically in skeleton forming cells

To identify putative skeletogenic genes and other unknown targets of the FGF signalling pathway, we conducted a transcriptome-wide analysis of SU5402-treated embryos relative to controls (Fig. 5). In this analysis we used a log fold change threshold of ±1.6 log2(SU5402/DMSO), as used for sea urchin (59,60), to select up- or down-regulated candidates in the transcriptome dataset (61). With this threshold, we obtained 140 downregulated and 2,366 upregulated transcripts (Fig. 5A). As SU5402 inhibited skeleton development (Fig. 2B), we focused our attention on the downregulated genes to pinpoint potential candidates that may be involved in skeleton formation. In the 140 downregulated transcripts, and using our transcriptome annotation (34), we found 101 sea urchin homologs of which only three were TFs (transcription factors; *Afi-six1/2, Afi-egr* and *Afi-soxD1*) and 16 were known skeletogenic genes (Fig. 5C). To improve the power of our predictions and to validate the differential transcriptome analysis, we performed NanoString on 123 selected candidates (26/140 downregulated,

5/2366 upregulated and other genes potentially involved in regeneration and development of skeleton; Table S4 and S5) on two biological replicates, and QPCR on three biological replicates using a subset of these 123 candidates. In order to compare data across different technologies, quantitative data were collected on the same sample using all three technologies (RNA-seq, QPCR and NanoString) and used to identify conversion factors to bring all data from different biological replicates on a comparable quantitative scale (details in Methods and Fig. S10). With this approach we were also able to compute additional significance values. 24 genes showed significant differences from 0 ($p^*<0.05$) of which 12 were below log2(fc) -1.6 and 3 above +1.6, and the residual 9 were close to ±1.6 (Fig. 5C). Interestingly, in the embryo only a few transcription factors were affected in the transcriptome-wide analysis and none of them are known TFs expressed in the SM. On the contrary, FGF and VEGF signalling components showed significant differential expression: both the two receptors specifically expressed in SM cells (*Afi-fgfr2* and *Afi-vegfR*) are down regulated in SU5402 treated embryos, while the *Afi-vegf2* ligand is upregulated (although with its regular low expression this might be an artifact; Table S2 and S3). To address the spatial expression of differentially expressed transcripts, we performed WMISH on selected genes from another biological replicate (Fig. 5B). WMISH on four downregulated transcripts specifically expressed in SM cells (*Afi-msp130L, Afi-tetraspanin*, *Afi-tr9107, Afi-slc4a10),* and one ectodermally-expressed gene *Afi-egr,* consistently showed loss of expression in SU5402-treated samples, whereas an increase in ubiquitous expression of *Afi-alx/arx* was detected, a gene identified as upregulated in all our quantitative expression assays. As a negative control

the unaffected gene *Afi-αcoll* shows no change of expression (Fig. 5B). These data indicate that the combination of different technologies on different biological replicates resulted in a reliable list of candidate genes that were affected by SU5402.

Molecular effects downstream of FGF signalling in embryogenesis and regeneration

To compare the genes transcriptionally regulated by FGF signalling between development and regeneration we performed a large-scale analysis of the effects of SU5402 perturbation in explants using NanoString. We used a code set of 123 genes and quantified 3 biological replicates of RNA extracted from 10 individual arm explants treated with SU5402 for 24h (at stage 2) relative to controls. To detect differentially expressed candidates a log fold change of 1 was used as a threshold of significance, similarly to previously published work (62). In this analysis we found 25 differentially expressed genes (10 upregulated and 15 downregulated). Since many candidates were found to be close to a fold change of ±1, we additionally assessed statistical significance using the Student's t-test. We found 23 differentially expressed genes of which 7 were shared between the threshold and t-test. Due to the small overlap, not even 50%, we compared the distributions of standard deviations between arms and embryos. We found a higher dispersion in the samples collected from arms than in the samples from embryos (Fig. S11). A possible explanation for such a high variance may be that arm samples are more heterogeneous and also contain only a small proportion of skeletogenic cells, thus increasing the noise-to-signal ratio and

making it more difficult to find affected genes using standard quantitative approaches.

To address whether the molecular effects of FGF signalling on skeleton development are similar between embryonic development and arm regeneration, we quantitatively compared the expression of various genes in the two processes. Of the 123 genes quantified using NanoString technology we found 24 in arm and 15 in embryo to be expressed below background (<20 counts comparable to internal negative control of the NanoString). Using the threshold of log2(SU5402/DMSO) ±1 for a better comparison, we find that overall 73 differentially expressed transcripts show the same trend of expression between arms and embryos, with 59 downregulated (Fig. S12A) and 14 upregulated (Fig. S12B). 22 genes show a different trend of expression (Fig. S12C). We performed WMISH on at least three SU5402-treated explants and relative controls for each gene from a selected group of transcripts (Fig. S13) to validate our quantitative analysis (Fig. 6). Transcripts classified as downregulated, specifically *Afi-egr, Afi-msp130L* and *Afi-slc4a10* show loss of expression in their respective territories (Fig. S13). *Afi-p58b* consistently showed no change of expression quantitatively or qualitatively (Fig. S13). Interestingly, *Afi-msp130L* is not part of the overlapping genes in the quantitative dataset but clearly showed no expression in SU5402 treated arms nor embryos by WMISH (Fig. 5 and Fig. S13), suggesting that our approach may be too stringent to detect all downregulated genes, especially in the more heterogeneous context of arm regeneration. Notably, we didn't observe any expression changes in cyclin genes (e.g. *cycA, cycD*) in SU5402-treated regenerates, in agreement with the EdU analysis showing cell

proliferation is not affected (Fig. 4). Additionally, three transcripts, homologs to the uncharacterised sea urchin tyrosine kinase *Afi-tk8/Cad96a, Afi-vegf2* and the homeodomain transcription factor *Afi-alx/arx*, are all upregulated in SU5402-treated embryos and adult regenerates (Fig. 6), although *Afi-vegf2* and *Afi-tk8/Cad96a* have very low, almost undetectable, expression levels in normal embryonic development (Table S2). Interestingly, few genes differentially affected by SU5402 relative to controls in the adult regenerating arms, but not in the embryos (Fig. 6), are stem cell-related transcription factors such as *Afi-runt1* and *Afi-fos,* and signalling genes belonging to other pathways (such as *Afi-serrate*). Importantly, upstream skeletogenic specification transcription factors (such as *Afi-alx1, Afi-ets1/2* and *Afi-jun*), as well a few downstream skeletogenic genes (*Afi-p19*, *Afi-*α*coll* and *Afi*-c-*lectin*) (33, 34) are unaffected by FGF signalling inhibition in both embryos and adults (Fig. 6 and Fig. S12). Notably, although the signalling genes *Afi-fgf9/16/20* and *Afi-fgfr2* are expressed in comparable cell types between regeneration and development (see Fig. 1), we find *Afi-fgfr2* to be downregulated only in the embryo and *Afi-fgf9/16/20* to be downregulated only in the arm, suggesting differences in regulatory processes activating the FGF signalling components during the two processes. Finally, in both embryos and regenerating arms, FGF signalling inhibition affects the expression of VEGF signalling genes: *Afi-vegf2* is upregulated, and *Afi-vegfr* is mildly downregulated. This suggests a potential mechanism of cross-talk between the two signalling pathways.

A new set of SM specific genes are found to be affected by FGF signalling inhibition

Impairing FGF signalling severely affects development and regeneration of the skeleton in *A. filiformis*. The data in the previous sections show that a large portion of known skeletogenic genes (such as *p58a*, *kirrell*, *msp130L*) require FGF signalling to be expressed in SM cells, therefore the differential transcriptome analysis conducted on embryos treated with SU5402 can be used to identify novel downstream genes involved in the development of skeleton in *A. filiformis*. Indeed, among the 140 downregulated genes, many (27 genes) do not have a clear homolog in the sea urchin genome, used as reference for annotation. BLAST analysis, shows that a handful of these transcripts have similarities with hemichordates or cnidarian genes (Table S7), 11 of them were included in the NanoString codeset and analysed for their expression and response to FGF signalling inhibition in embryos and regenerating arms. Nine of these new *A. filiformis* genes show a similar response to SU5402 exposure in both the embryo and regenerating arms (Fig. S12). Bioinformatic analysis on five of these novel genes revealed that *Afi-tr31926* and *Afi-tr35695* are unique to brittle stars (also found in *Ophiocoma wendtii*) with no similarity to other sequences within analysed echinoderms (BLAST using Echinobase/EchinoDB databases) or in other organisms (NCBI non-redundant database) (Table S7). Protein structure prediction using PredictProtein (63) and analysis of conserved domains using CDART and PFAM databases revealed that these genes are likely to be secreted (presence of a signal peptide) and one of those (*Afi-tr35695*) is predicted to have calcium ion binding activity, which would be consistent with

its putative role in the formation of a calcium carbonate skeleton (Table S7). WMISH show that *Afi-tr31926 and Afi-tr35695* are indeed expressed in the skeletogenic mesoderm in both the embryo and in the regenerating arm, either in early stages, late stages or both (Fig. S14). *Afi-tr9107,* on the other hand*,* is expressed in the ectoderm in a pattern that is reminiscent of the expression of the signalling ligands *Afi-fgf9/16/20* and *Afi-vegf3* in the ectoderm of the embryo at the boundary with the endoderm (Fig. 5), adjacent to where the skeleton is deposited. During regeneration this transcript is expressed in vertebrae and spines of late regenerating adult arms (Fig. S14).

Interestingly, in our analysis we also found two new genes, which have not been previously described to have expression in SM cells in sea urchin. One is the transcription factor *Afi-rreb1*, not consistently downregulated in different biological replicas, and the gene *Afi-cara7la* (Fig. 5C) consistently downregulated in SU5402-treated embryos. Both are specifically expressed in the skeletogenic territory in both embryos and regenerating arms (Fig. S13) and constitute additional novel skeletogenic genes identified in this study.

Altogether, these data identify new genes downstream of FGF signalling, and similarities in the molecular network driving skeletogenesis between embryonic development and adult arm regeneration, suggesting that they are functionally equivalent.

Discussion

FGF signalling is required for skeleton formation in the brittle star and activates a cassette of biomineralization genes

In this work we show that both brittle star skeletal development and adult regeneration rely heavily on the presence of FGF signalling. The evidence for this is as follows: 1) the expression pattern of *FGF* and *VEGF* ligands and receptors during development and regeneration allows for the ectodermal-mesodermal tissue interaction, which has been shown to be crucial for skeletogenesis in sea urchin embryos (29–32); 2) perturbation of this pathway using the universal pharmacological agent SU5402 resulted in complete inhibition of skeletal spicule formation in both adult arms and embryos; and 3) FGF signalling inhibition specifically downregulated the expression of genes involved in biomineralization. Similarly to what was suggested for sea urchins (29), we show that the role of FGF signalling during skeletogenesis in the brittle star appears to be confined to downstream differentiation of skeletogenic cells, as putative upstream transcription factors (e.g. *Afi-alx1, Afi-ets1/2*) are unaffected. The observed effect on skeletal downstream genes, such as *msp130*, *slc4a10, kirrell* and more, rather than transcriptional regulators, suggest a role of FGF signalling primarily in the differentiation step of skeleton development rather than in specification.

Proteomic studies have revealed hundreds of proteins associated with both the sea urchin and brittle star skeletal matrices (64,65). Interestingly, FGF signalling perturbation downregulated only a subset of those

skeletogenic differentiation genes, while having no effect on others (e.g. *Afi-p19, Afi-c-lectin*). Nevertheless, this subset of downregulated genes is essential for skeleton formation as their collective downregulation results in the failure of the last checkpoint in the skeletogenesis network – deposition of the biomineralized skeleton by mesenchymal cells. Those include genes belonging to the carbonic anhydrase gene family (e.g. *cara7la)*, implicated in calcium carbonate deposition in various organisms including sea urchins (66,67) and molluscs (68), solute carrier proteins like *slc4a10*, and mesenchymal surface glycoproteins like *msp130* (69).

Functional conservation of FGF signalling in embryonic and regenerative skeletogenesis

A molecular conservation of genes expressed during embryonic development and regeneration was previously shown in newts (3) and chick embryos (4). However, these studies were limited to a comparison of only one or a few genes. Most recently, the transcriptomes of the embryo and regenerating stages of the sea anemone, *Nematostella vectensis*, have provided the first large-scale resource for comparing those two processes at global level and also revealed important differences between them (9). It is thus of great interest to compare specific aspects of development between embryogenesis and regeneration, for instance similar cell types or structures. Our previous work has already shown that the morphology and molecular signature of skeletogenic cells is highly similar between the embryo and regenerating adult arm of *A. filiformis* (33,35,36). The importance of FGF signalling in skeleton development and regeneration in *A. filiformis* reveals additional functional

similarities between skeletogenesis at both stages of the brittle star life cycle. Figure 7 summarizes the underlying provisional molecular network downstream of FGF signalling in skeletal cells. It is highly conserved between regeneration and development, with several genes being specifically downregulated in both cases e.g. the biomineralization genes *Afi-kirrelL, Afi-msp130L* and *Afi-slc4a10*. Few key changes, however, are also revealed in our work: 1) differential response of FGF signalling components (*fgf19/16/*20 and *fgfr2*) to the SU5402 treatment in the two processes; 2) ectodermal expression of the gene *tr9107*; and 3) the skeletal gene *p58*. Taken together, our data provides support for the hypothesis of regeneration re-capitulating development, at least at the level of cell differentiation, and provides a large-scale comparison of the molecular networks driving development and regeneration of the same cell type in the same species. It remains to be found whether the initiating molecular events upstream of this signalling pathway are also conserved or significantly different as suggested by other studies (10).

Cross-talk between FGF and VEGF signalling regulatory networks

It has been previously suggested that the FGF and VEGF signalling pathways may function synergistically, whereby the downregulation of either of the ligands can affect the expression of the other pathway components (30,70). For instance, specifically in sea urchins, downregulation of *fgf19/16/*20 (also called *fgfa)* results in upregulation of *vegf3* expression, while downregulation of *vegf3* results in upregulation of *fgfr2* (30). Our analysis of downstream targets of the FGF pathway provides insights into the mechanisms of its transcriptional regulation in *A. filiformis*. Our results show that the inhibition of

FGF signalling in skeletal cells impinges on the expression of VEGF pathway genes downregulating the receptor *Afi-vegfr,* expressed in skeletogenic cells. Moreover, SU5402 induces upregulation of the *Afi-Vegf2* ligand gene that has very low expression in controls embryos (Fugure S7). This is consistent with the very dramatic phenotype observed in the FGF inhibition experiments, which ultimately will affect also the VEGF signalling in these cells. This highlights how the two signalling pathways are interlinked not only in the sea urchin but also in the brittle star, albeit in a different manner. However, this presence of signalling cross talk underlines the difficulty with dissecting the roles of signalling pathways, which may be tightly linked to inter-regulatory and feed-back loops, suggesting the presence of a signalling network in which ligands and receptors are under the control of other signalling pathways.

Evolution of FGF signalling and skeleton formation in echinoderms

The evolution of the FGF gene family involved extensive gene duplication and gene loss, often lineage-specific (71), resulting in complex and variable distribution of FGF genes among metazoans. In vertebrates, major duplications of the gene family occurred resulting in 19 FGFs in chicken and over 22 FGFs in mammals (71,72). There are far fewer receptors of the pathway with only four functional FGFR genes in vertebrates (73), two in sea urchins (46) and two in *Drosophila* (73). Only one Fgf ligand has been described in sea urchins, whereas hemichordates have five ligands (48), some of which result from specific duplications within the Ambulacraria. In *A. filiformis* we identified 2 Fgf ligands and 2 Fgf receptors, suggesting that gene

independent duplication events from a common ancestral FGF ligand and receptor occurred in chordates as well as in echinoderms.

In sea urchin embryos, FGF signalling components are expressed in a complimentary pattern, whereby the *fgfr2* receptor is specifically expressed by the SM cells and the *fgf9/16/20 (or fgfa)* ligand is expressed in overlying ectoderm (29,30). Recent work showed that this pattern of expression is also observed for the VEGF signalling genes in both sea urchin (30–32) and brittle stars embryos, as well as in sea urchin and sea star juveniles (74,75). It has been suggested that the heterochronic activation of this pathway in sea urchin and brittle star embryos lead to the co-option of the adult skeleton into the larva (74,76), as sea star embryos do not have those genes expressed at the embryonic stage and have no larval skeleton (74). Our results show that both VEGF and FGF genes are expressed in a strikingly similar pattern in embryos and adult regenerating arms of *A. filiformis,* suggesting that the interaction of the skeletogenic cells with the ectoderm, mediated by those signalling pathways, may be a conserved feature for adult echinoderms, and has in fact been co-opted in the embryos of sea urchins and brittle stars to form a larval skeleton. Our data suggests that in brittle stars FGF signalling plays a more prominent role in skeletogenesis than VEGF signalling, which is the opposite case for sea urchins (30). Furthermore, the transcriptional regulation downstream of FGF signalling appears to be significantly different in brittle stars and sea urchins, namely: 1) approximately 30% of genes identified in our differential screen did not have sea urchins homologs (e.g. *tr31926, tr35695*); 2) other genes with homologs are not specifically expressed in the skeletogenic lineage in the sea urchin (e.g. *Afi-rreb1;* (77)*)*. Recent work

showed that despite a striking similarity in the morphology and development of the larval skeleton in sea urchins and brittle stars, the dynamics of their regulatory states are very different, suggesting alternative re-wiring of the network in the two classes (33). Together with our results showing the high degree of conservation of the brittle star embryonic and adult network downstream of FGF signalling, we can hypothesize that the embryonic program for skeletogenesis could have been independently co-opted in brittle stars and sea urchins. An alternative evolutionary scenario would imply a coordinated evolution of the skeletogenic program in larvae and adults. Elucidating the role of FGF signalling in adult skeletogenesis of the remaining four classes of extant echinoderms could help resolve this issue in the future.

Evolutionary implications for skeletogenesis among deuterostomes

Skeletal regeneration is observed in other deuterostome groups: for example in cirri regeneration of amphioxus (78), and in appendage regeneration of different vertebrates (reviewed in (79)). It has even been suggested that adult bone repair and regeneration may recapitulate embryonic bone development at a molecular level (80). Comparing the skeleton developmental program between embryogenesis and regeneration can be vital to understand the evolution of skeletogenesis in deuterostomes. Although the skeleton of echinoderms is composed of calcium carbonate, instead of calcium phosphate, similarities of its ontogeny can be observed when compared to vertebrates. For example, in both groups the trunk skeletal precursor cells are mesoderm-derived, motile mesenchymal cells. Gene expression can also aid in understanding the extent of potential similarities.

The key regulators of the sea urchin (and likely brittle star) skeletogenic GRN include transcription factors *alx1*, *ets1/2* and *erg* (33,35,37,83–85). Members of the Cart/Alx3/Alx4 group of TFs are also involved in skeletal development in vertebrates. They are expressed in embryonic lateral plate mesoderm, limb buds, cartilage and ectomesenchyme, and deletions of these genes result in cranial and vertebral malformations (38,39,86). ETS family TFs (homologs of *ets1/2* and *erg*) have also been implicated in vertebrate skeletogenesis (87–92). FGF signalling has a highly conserved role in skeletogenesis in deuterostomes, as demonstrated in sea urchins (29), lampreys (93), chickens (94) and mice (95,96).

In terms of downstream biomineralization genes, the network has diverged significantly between echinoderms and vertebrates. Most of the biomineralization genes identified in sea urchins and brittle stars do not have apparent homologues in vertebrates or other invertebrate deuterostomes (33,65,67). Interestingly, the recent genome of the brachiopod *Lingula anatine*, which like distantly related vertebrates forms its shell using calcium phosphate, also reveals a unique expansion of a set of biomineralization genes (for example chitin synthases) different from duplication events which gave rise to bone formation genes in vertebrates (such as fibrillar collagens) (97). Those differences in the set of biomineralization genes used by brachiopods, echinoderms and vertebrates suggest that these animals independently evolved a core differentiation gene cassette via duplication events for building their calcium-based skeletons. Nevertheless, the initiation cascade, including the ancient signalling pathways (e.g. FGF, BMP) and transcription factors, appears to play a conserved role in these divergent

animals (67,97–100). Together with these studies, our work presents further evidence for an evolutionary conserved regulatory apparatus driving the activation of biomineralization genes.

Conclusions

In this study, we present a comparison of the role of FGF signalling in the embryonic development and adult regeneration of the skeleton in the brittle star *Amphiura filiformis*. We characterized the expression of FGF and VEGF signalling pathway ligands and receptors during both embryonic development and adult arm regeneration. Using the inhibitor SU5402 we showed that perturbation of FGF signalling interferes with skeleton formation during both developmental processes. Our transcriptome-wide analysis of the effects of FGF signalling inhibition in brittle star embryos revealed a global view of the downstream targets of this pathway, including well-studied genes and novel brittle star skeletogenic genes. Finally, our comparative analysis of these FGF targets between embryos and adult regenerating arms strongly supports a high degree of conservation of the downstream molecular network underlying skeletogenesis. Although many processes are highly divergent between development and regeneration, such as wound healing and initial cellular organization, identification and comparison of the upstream signals activating the skeletogenic GRN in embryos and adults will elucidate whether regeneration truly re-capitulates development at the level of cell type specification and differentiation. This comparative work on skeletal development will also contribute to our understanding of the evolution of skeletogenesis within both echinoderms and deuterostomes more broadly.

Materials and Methods

Adult animal maintenance and handling

Adult animals of *Amphiura filiformis* were collected during their reproductive season (July-August) for embryo cultures and throughout the year for adult specimens in the Gullmarsfjord, Sweden in the proximity of the Sven Lovén Centre for Marine Sciences. Animals were maintained in the laboratory in London as described previously (35). Regenerating arm samples were obtained as described (36) while amputated arm explants were obtained as described in Burns et al., 2012. *A. filiformis* embryo culture was set up as previously described (101). Treated and untreated embryos were collected at required stages for WMISH, RNA extraction and RNAseq as previously described (33,34). Arm regeneration experiments were conducted on animals of similar size, as an indication of similar age and with similar regeneration dynamics (102). Specifically, for non-regenerating arms one segment was cut from each arm. Similarly, for stage 1 arms at different time points (24hpa, 48hpa, 72hpa) only the last segment before the amputated site was collected. For stages 3-5 only the regenerating bud was collected with no additional stump tissues. Finally, for the 50% DI stage arms five segments from the proximal side of the regenerate closest to the stump and five segments from the distalmost side (excluding the distal cap) were collected corresponding to the most undifferentiated tissues (Fig. S6).

Whole mount in situ hybridization

The protocol for WMISH for embryos and adult regenerating arms of *A. filiformis* was identical except for the hybridization temperature as outlined below. The samples were first re-hydrated with graded ethanol washes (70%, 50% and 30%) and washed three times in 1x MA Buffer with Tween (MABT; 0.1M Maleic Acid pH 7.5, 0.15M NaCl, 0.1% Tween-20) and pre-hybridized in hybridization buffer (50% deionized formamide, 10% PEG, 0.05M NaCl, 0.1% Tween-20, 0.005M EDTA, 0.02M Tris pH 7.5, 0.1mg/ml yeast tRNA, 1x Denhart's solution, DEPC-treated water) for 1h at 50°C (regenerating arms) or 55°C (embryos). Next, the samples were put in HB containing 0.2ng/ μ l antisense probe for 3-7 days at the same temperature. Following this period of time samples were post-hybridized in fresh HB without probe for three hours, then washed once in MABT at the corresponding hybridization temperatures and once at room temperature (RT). The samples were then washed three times in 0.1x MABT, once more with 1x MABT before placing them in blocking solution (MABT, 0.5% goat serum) for 30 min. Samples were then incubated in 1:1000 anti-DIG AP (Roche) antibody solution overnight at 4°C. Next, the sample was washed 5 times in 1x MABT and 2 times in alkaline phosphatase (AP) buffer (Tris pH 9.5, $MgCl_2$, NaCl, Tween-20, levamisole, milliQ water) before adding the staining solution (AP buffer, 10% DMF, 2% NBT/BCIP) for the chromogenic detection. The staining was stopped with MABT washes.

Inhibitor treatments and phenotypic analysis

SU5402 (Calbiochem) and Axitinib (Sigma) were dissolved in DMSO for a stock concentration of 10mM and 5mM respectively. The drugs were added to embryo cultures at 18hpf at a final concentration of 10μM (SU5402) and 75nM (Axitinib), and the embryos were then allowed to develop until 27hpf. At this time-point approximately 500 treated and control (0.2% DMSO and FSW) embryos were collected for fixation for *in situ* hybridization and 500 embryos were collected for RNA extraction for QPCR and NanoString analysis. Remaining embryos were left to develop further for phenotypic assessment. Arm explants were used for testing the effects of inhibitors on regeneration and skeletogenesis. Adult *A. filiformis* arms were cut 1 cm from the disc and then left to regenerate until stage 2 (on average 5 days post-amputation). Arms were then cut again 5mm proximally to the initial amputation site to obtain explants, which were left for several hours to allow proximal wound healing. The explants were then incubated for 24h in SU5402 at a final concentration of 10μM or Axitinib at 200nM. Samples reared in FSW and 0.1% DMSO were used as controls. The development of biomineralized skeletal primordia (or spicules) was monitored by incorporation of calcein (Sigma; 1:50 dilution of a 1.25mg/ml stock solution), a green fluorescent dye that labels the newly deposited $CaCO_3$ (55). . After the treatment, the arm explants were imaged for any morphological phenotype and fixed for WMISH or collected in RLT (15 arms pooled together per condition) for NanoString analysis.

Differential analysis of transcriptome data

Samples were quantified and normalized as previously described (34). Differential analysis was conducted between SU5402 and DMSO treated samples. Since only one biological replicate was used for mRNA-seq, we used it to identify potentially differentially expressed candidates and validated those using other technologies. Candidates were selected based on two criteria: (1) a user defined threshold of expression above 2 tpm and (2) a fold-change threshold of +-1.6.

Since all three methods (transcriptome quantification, NanoString and QPCR) employ technologically different quantification strategies, we assessed their technical similarity by comparing fold change values of the different methods on the same biological replicate. Consistently, all three technologies showed a similar trend in fold change (88.1%). Transcriptome and NanoString fold change values for 114 genes showed high positive correlation (~0.85) and linear regression analysis resulted in a significant positive association between the two techniques (β=1.12, 95% CI [0.97, 1.24], p***<0.001, adjusted R^2=0.7223; S6 Fig). Interestingly, fold change values seemed generally slightly inflated in the transcriptome dataset (slope > 1). When comparing fold change values of 31 genes between QPCR and Transcriptome we found a positive correlation (~0.854) and that both techniques are positively associated (β=1.4340, 95% CI [1.10, 1.77], p***<0.001, adjusted R^2=0.7203; S6 Fig). This is consistent with our observation comparing correlations of time-course datasets quantified using transcriptomics, NanoString and QPCR (34). Importantly, since every technology encompasses differences in their technical error, we used the β

and y-intersect values of the linear regression analysis to compare biological replicates across technologies.

Inference of phylogenetic gene trees

For phylogenetic gene trees, sequences were collected from local assemblies and publicly available datasets (41 species). To fish out genes that contained the FGF, FGFR, VEGF and VEGFR domains, we obtained HMM profiles from the PFAM database. The sequences of the 41 species were scanned against these domains and were used to generate input data for OMA (v2.2.0) (103). Hierarchical orthologous groups that contained our candidates were merged with groups that showed close blast similarity and were selected for further analysis. The merging step was necessary due to the independent divergence between chordates and echinoderms of more than 500 Mya (million years ago) and still too low taxonomic sampling. Mafft (v7) (104) was used for multiple sequence alignment, followed by several manual rounds of sequence trimming using maxAlign (v1.1) (105) or independent criteria such as retention of close sequence length to given candidate. For tree inference we used Iqtree (v.1.5.5) with LG model and 1000 fast bootstraps (106).

Validation of differentially expressed candidates using QPCR and NanoString

To validate candidates obtained from the transcriptome analysis we performed a linear regression analysis between transcriptome vs QPCR and transcriptome vs NanoString using R. Coefficients obtained for slope and y-intercept were used to scale QPCR and NanoString samples in relation to the

transcriptome. In this way, we accommodate differences in intrinsic technical errors of the various technologies.

QPCR and NanoString nCounter analysis

QPCR analysis was performed as described previously for adult regenerating arms (35) and embryonic samples (33). Additionally, differential expression of genes was measured using the NanoString nCounter analysis system (NanoString Technologies, Seattle, WA, USA) (107). A 123-probe code set was designed based on *A. filiformis* sequences, including six different internal standard genes and a GFP probe for detecting spike-in GFP RNA (Table S4). For each experimental sample 100ng of total RNA was used, extracted from 300 embryos and 10 regenerating arms respectively, using the RNeasy Micro Kit (Qiagen). Detected counts/100ng of total RNA were normalized first using the positive control lane normalization provided in the NanoString nCounter cartridge and then again using selected six internal standard genes (normalization factor obtained using geometric mean for each lane). For quantifying differential gene expression in perturbed samples, a Log2 fold change between controls and treated samples was calculated. The Log2(SU5402/DMSO) of ±1 (reflecting a 2-fold difference in change of level of expression) was determined to be biologically significant in correspondence with previously published work (62).

Cell proliferation assay

Regenerates treated with the SU5402 inhibitor were tested for changes in cell proliferation. The cell proliferation assay was carried out using the Click-iT® EdU HCS Assay (Invitrogen) as described previously (36) then imaged using confocal microscopy. For each regenerate between ~100 ±10 slices were taken per Z-stack (1µm thickness). DAPI-labelled nuclei and EdU-Labelled nuclei per stack were counted automatically using the Fiji plugin TrackMate (108). Number of EdU labelled nuclei per total number of nuclei ranged from 672/3375 to 1385/5205. The proportion of nuclei labelled with EdU compared to all nuclei labelled with DAPI was calculated as a percentage. Student's T-test was used and showed no significant difference between control (DMSO) and SU5402-treated samples (T-value = 0.261; $p>0.25$).

Acknowledgments

We would like to thank the staff at the Sven Lovén Centre for Marine Sciences in Kristineberg, especially Sam Dupont, for assistance during animal and sample collection. We thank Olga Ortega-Martinez for sharing the regenerating explant collection method. We thank Sheida Rezaee and Emanuele Astoricchio for assistance in cloning and WMISH. We would like to thank Jeffrey Thompson, Johannes Girstmair and Maria Kotini and anonymous reviewers for helpful comments on the manuscript.

Competing interests

The authors declare no competing interests.

Author contributions

AC, DVD and PO conceived and designed the experiments. AC, DVD, PO and LC carried out experiments. AC, DVD and PO analysed the data. AC, DVD and PO wrote the manuscript.

Funding

This work was partly funded by the KVA fund SL2015-0048 from the Royal Swedish Academy of Science and the EU FP7 Research Infrastructure Initiative ASSEMBLE (ref. 227799). AC was funded by a Wellcome Trust PhD fellowship grant (099745/Z/12/Z). DVD was funded by a Systems Biology UCL studentship and by a Swiss National Science Foundation grant (150654).

References

1. Brockes JP, Kumar A. Comparative aspects of animal regeneration. Annu Rev Cell Dev Biol. 2008;24:525–49.
2. Morgan TH. Regeneration. Columbia Univ Biol Ser VII. 1901;342.
3. Imokawa Y, Yoshizato K. Expression of Sonic hedgehog gene in regenerating newt limb blastemas recapitulates that in developing limb buds. Proc Natl Acad Sci U S A. 1997;94(17):9159–64.
4. Ozpolat BD, Zapata M, Fruge JD, Coote J, Lee J, Muneoka K, et al. Regeneration of the elbow joint in the developing chick embryo recapitulates development. Dev Biol. 2012;372(2):229–38.
5. Mercader N, Tanaka EM, Torres M. Proximodistal identity during vertebrate limb regeneration is regulated by Meis homeodomain proteins. Development. 2005;132(18):4131–42.
6. Pineda D, Rossi L, Batistoni R, Salvetti A, Marsal M, Gremigni V, et al. The genetic network of prototypic planarian eye regeneration is Pax6 independent. Development. 2002;129(6):1423–34.
7. Saló E, Pineda D, Marsal M, Gonzalez J, Gremigni V, Batistoni R. Genetic network of the eye in Platyhelminthes: Expression and functional analysis of some players during planarian regeneration. Gene. 2002;287(1–2):67–74.
8. Matsunami M, Suzuki M, Haramoto Y, Fukui A, Inoue T, Yamaguchi K, et al. A comprehensive reference transcriptome resource for the Iberian ribbed newt Pleurodeles waltl , an emerging model for developmental and regeneration biology. DNA Res. 2019;26(3):217–29.

9. Warner JF, Guerlais V, Amiel AR, Johnston H, Nedoncelle K, Röttinger E. NvERTx: a gene expression database to compare embryogenesis and regeneration in the sea anemone Nematostella vectensis. Development. 2018;145(10):dev162867.
10. Warner JF, Amiel AR, Johnston H, Röttinger E. Regeneration is a partial redeployment of the embryonic gene network. bioRxiv. 2019;
11. Thisse B, Thisse C. Functions and regulations of fibroblast growth factor signaling during embryonic development. Dev Biol. 2005;287(2):390–402.
12. Dorey K, Amaya E. FGF signalling: diverse roles during early vertebrate embryogenesis. Development. 2010;137(22):3731–42.
13. Poss KD, Shen J, Nechiporuk A, McMahon G, Thisse B, Thisse C, et al. Roles for Fgf signaling during zebrafish fin regeneration. Dev Biol. 2000;222:347–58.
14. Lee Y, Grill S, Sanchez A, Murphy-Ryan M, Poss KD. Fgf signaling instructs position-dependent growth rate during zebrafish fin regeneration. Development. 2005;132(23):5173–83.
15. Lin G, Slack JMW. Requirement for Wnt and FGF signaling in Xenopus tadpole tail regeneration. Dev Biol. 2008;316(2):323–35.
16. Makanae A, Mitogawa K, Satoh A. Co-operative Bmp- and Fgf-signaling inputs convert skin wound healing to limb formation in urodele amphibians. Dev Biol. 2014;396(1):57–66.

17. Shibata E, Yokota Y, Horita N, Kudo A, Abe G, Kawakami K, et al. Fgf signalling controls diverse aspects of fin regeneration. Development. 2016;143:2920–9.

18. Turwankar A, Ghaskadbi S. VEGF and FGF signaling during head regeneration in hydra. Gene [Internet]. 2019;717(August):144047. Available from: https://doi.org/10.1016/j.gene.2019.144047

19. Cunningham M, Seto M, Ratisoontorn C, Heike C, Hing A. Syndromic craniosynostosis : from history to hydrogen bonds. Orthod Craniofacial Res. 2007;10:67–81.

20. Marie PJ, Coffin JD, Hurley MM. FGF and FGFR signaling in chondrodysplasias and craniosynostosis. J Cell Biochem. 2005;96(5):888–96.

21. Roscioli T, Flanagan S, Kumar P, Masel J, Gattas M, Hyland VJ, et al. Clinical findings in a patient with FGFR1 P252R mutation and comparison with the literature. Am J Med Genet. 2000;93(1):22–8.

22. Teven CM, Farina EM, Rivas J, Reid RR. Fibroblast growth factor (FGF) signaling in development and skeletal diseases. Genes Dis. 2014;1(2):199–213.

23. Schmid G, Kobayashi C, Sandell L, Ornitz DM. Fibroblast Growth Factor expression during skeletal fracture healing in mice. Dev Dyn. 2009;238(3):766–74.

24. Du X, Xie Y, Xian CJ, Chen L. Role of FGFs/FGFRs in skeletal development and bone regeneration. J Cell Physiol. 2012;227(12):3731–43.

25. Oliveri P, Tu Q, Davidson EH. Global regulatory logic for specification of an embryonic cell lineage. Proc Natl Acad Sci U S A. 2008;105:5955–62.

26. Davidson EH, Rast JP, Oliveri P, Ransick A, Calestani C, Yuh C-H, et al. A provisional regulatory gene network for specification of endomesoderm in the sea urchin embryo. Dev Biol. 2002;246(1):162–90.

27. Peter IS, Davidson EH. The endoderm gene regulatory network in sea urchin embryos up to mid-blastula stage. Dev Biol. 2010;340:188–99.

28. Annunziata R, Arnone MI. A dynamic regulatory network explains ParaHox gene control of gut patterning in the sea urchin. Development. 2014;141(12):2462–72.

29. Röttinger E, Saudemont A, Duboc V, Besnardeau L, McClay D, Lepage T. FGF signals guide migration of mesenchymal cells, control skeletal morphogenesis and regulate gastrulation during sea urchin development. Development. 2008;135:353–65.

30. Adomako-Ankomah A, Ettensohn CA. Growth factor-mediated mesodermal cell guidance and skeletogenesis during sea urchin gastrulation. Development. 2013;140(20):4214–25.

31. Duloquin L, Lhomond G, Gache C. Localized VEGF signaling from ectoderm to mesenchyme cells controls morphogenesis of the sea urchin embryo skeleton. Development. 2007;134:2293–302.

32. Erkenbrack EM, Petsios E. A Conserved Role for VEGF Signaling in Specification of Homologous Mesenchymal Cell Types Positioned at Spatially Distinct Developmental Addresses in Early Development of Sea Urchins. J Exp Zool Part B Mol Dev Evol. 2017;328B:4243–432.

33. Dylus DV, Czarkwiani A, Stångberg J, Ortega-Martinez O, Dupont S, Oliveri P. Large-scale gene expression study in the ophiuroid Amphiura filiformis provides insights into evolution of gene regulatory networks. Evodevo. 2016;7(1):2.

34. Dylus D V., Czarkwiani A, Blowes LM, Elphick MR, Oliveri P. Developmental transcriptomics of the brittle star Amphiura filiformis reveals gene regulatory network rewiring in echinoderm larval skeleton evolution. Genome Biol. 2018;19(1):1–17.

35. Czarkwiani A, Dylus D V., Oliveri P. Expression of skeletogenic genes during arm regeneration in the brittle star Amphiura filiformis. Gene Expr Patterns. 2013;13:464–72.

36. Czarkwiani A, Ferrario C, Dylus D V., Sugni M, Oliveri P. Skeletal regeneration in the brittle star Amphiura filiformis. Front Zool. 2016;13:18.

37. Ettensohn CA, Illies MR, Oliveri P, De Jong DL. Alx1, a member of the Cart1/Alx3/Alx4 subfamily of Paired-class homeodomain proteins, is an essential component of the gene network controlling skeletogenic fate specification in the sea urchin embryo. Development. 2003;130(13):2917–28.

38. Brouwer A, ten Berge D, Wiegerinck R, Meijlink F. The OAR/aristaless domain of the homeodomain protein Cart1 has an attentuating role in vivo. Mech Dev. 2003;120:241–52.

39. ten Berge D, Brouwer A, el Bahi S, Guénet JL, Robert B, Meijlink F. Mouse Alx3: an aristaless-like homeobox gene expressed during embryogenesis in ectomesenchyme and lateral plate mesoderm. Dev Biol. 1998;199(1):11–25.

40. Delroisse J, Ortega-Martinez O, Dupont S, Mallefet J, Flammang P. De novo transcriptome of the European brittle star Amphiura filiformis pluteus larvae. Mar Genomics. 2015;23:109–21.

41. Purushothaman S, Saxena S, Meghah V, Swamy CVB, Ortega-Martinez O, Dupont S, et al. Transcriptomic and proteomic analyses of Amphiura filiformis arm tissue-undergoing regeneration. J Proteomics. 2014;1–12.

42. Burns G, Ortega-Martinez O, Thorndyke MC, Peck LS, Dupont S, Clark MS. Dynamic gene expression profiles during arm regeneration in the brittle star Amphiura filiformis. J Exp Mar Bio Ecol. 2011;407:315–22.

43. Cameron RA, Samanta M, Yuan A, He D, Davidson E. SpBase: The sea urchin genome database and web site. Nucleic Acids Res. 2009;37:750–4.

44. Finn RD, Coggill P, Eberhardt RY, Eddy SR, Mistry J, Mitchell AL, et al. The Pfam protein families database: Towards a more sustainable future. Nucleic Acids Res. 2016;44(D1):D279–85.

45. Altenhoff AM, Levy J, Zarowiecki M, Vesztrocy AW, Dalquen DA, Müller S, et al. OMA standalone : orthology inference among public and custom genomes and transcriptomes. Genome Reseach. 2019;29:1–12.

46. Lapraz F, Röttinger E, Duboc V, Range R, Duloquin L, Walton K, et al. RTK and TGF-β signaling pathways genes in the sea urchin genome. Dev Biol. 2006;300(1):132–52.

47. Sarabipour S, Hristova K. Mechanism of FGF receptor dimerization and activation. Nat Commun. 2016;7:10262.

48. Fan T-P, Su Y-H. FGF signaling repertoire of the indirect developing hemichordate Ptychodera flava. Mar Genomics. 2015;24:1–9.

49. Czarkwiani A, Ferrario C, Dylus DV, Sugni M, Oliveri P. Skeletal regeneration in the brittle star Amphiura filiformis. Front Zool. 2016;13(1).

50. Mohammadi M, McMahon G, Sun L, Tang C, Hirth P, Yeh BK, et al. Structures of the tyrosine kinase domain of fibroblast growth factor receptor in complex with inhibitors. Science. 1997;276(5314):955–60.

51. Saradamba A, Buch PR, Murawala HA, Balakrishnan S. SU5402, a pharmacological inhibitor of fibroblast growth factor receptor (FGFR), effectively hampers the initiation and progression of fin regeneration in teleost fish. Eur J Zool Res. 2013;2(4):1–9.

52. Hu D, Marcucio RS. Neural crest cells pattern the surface cephalic ectoderm during FEZ formation. Dev Dyn. 2012;241(4):732–40.

53. Eblaghie M, Simon L, Dickinson R, Munsterberg A, Sanz-Ezquerro J, Farrell E, et al. Negative Feedback Regulation of FGF Signaling Levels by Pyst1/MKP3 in Chick Embryos. Curr Biol. 2003;13:1009–18.

54. Burns G, Ortega-Martinez O, Dupont S, Thorndyke MC, Peck LS, Clark MS. Intrinsic gene expression during regeneration in arm explants of Amphiura filiformis. J Exp Mar Bio Ecol. 2012;413:106–12.

55. Guss KA, Ettensohn CA. Skeletal morphogenesis in the sea urchin embryo: regulation of primary mesenchyme gene expression and skeletal rod growth by ectoderm-derived cues. Development. 1997;124(10):1899–908.

56. Kipryushina YO, Yakovlev K V., Kulakova MA, Odintsova NA. Expression pattern of vascular endothelial growth factor 2 during sea urchin development. Gene Expr Patterns [Internet]. 2013;13(8):402–6. Available from: http://dx.doi.org/10.1016/j.gep.2013.07.003

57. Sun L, Tran N, Liang C, Tang F, Rice A, Schreck R, et al. Design, Synthesis, and Evaluations of Substituted 3-[(3- or 4-Carboxyethylpyrrol-2-yl)methylidenyl]indolin-2-ones as Inhibitors of VEGF, FGF, and PDGF Receptor Tyrosine Kinases. J Med Chem. 1999 Dec;42(25):5120–30.

58. Hu-Lowe DD, Zou HY, Grazzini ML, Hallin ME, Wickman GR, Amundson K, et al. Nonclinical antiangiogenesis and antitumor activities of axitinib (AG-013736), an oral, potent, and selective inhibitor of vascular endothelial growth factor receptor tyrosine kinases 1, 2, 3. Clin Cancer Res. 2008;14(22):7272–83.

59. Wei Z, Angerer RC, Angerer LM. A database of mRNA expression patterns for the sea urchin embryo. Dev Biol. 2006;300(1):476–84.

60. Weitzel HE. Differential stability of -catenin along the animal-vegetal axis of the sea urchin embryo mediated by dishevelled. Development. 2004;131(12):2947–56.

61. Materna SC, Oliveri P. A protocol for unraveling gene regulatory networks. Nat Protoc. 2008;3(12):1876–87.

62. Cui M, Siriwon N, Li E, Davidson EH, Peter IS. Specific functions of the Wnt signaling system in gene regulatory networks throughout the early sea urchin embryo. Proc Natl Acad Sci U S A. 2014;111(47):E5029-38.

63. Yachdav G, Kloppmann E, Kajan L, Hecht M, Goldberg T, Hamp T, et al. PredictProtein — an open resource for online prediction of protein structural and functional features. 2014;42(May):337–43.

64. Mann K, Wilt FH, Poustka AJ. Proteomic analysis of sea urchin (Strongylocentrotus purpuratus) spicule matrix. Proteome Sci. 2010;8:33.

65. Seaver RW, Livingston BT. Examination of the skeletal proteome of the brittle star Ophiocoma wendtii reveals overall conservation of proteins but variation in spicule matrix proteins. Proteome Sci. 2015;13(1):1–12.

66. Mann K, Poustka AJ, Mann M. The sea urchin (Strongylocentrotus purpuratus) test and spine proteomes. Proteome Sci. 2008;6:22.

67. Livingston BT, Killian CE, Wilt F, Cameron A, Landrum MJ, Ermolaeva O, et al. A genome-wide analysis of biomineralization-related proteins in the sea urchin Strongylocentrotus purpuratus. Dev Biol. 2006;300(1):335–48.

68. Mann K, Edsinger-Gonzales E, Mann M. In-depth proteomic analysis of a mollusc shell: acid-soluble and acid-insoluble matrix of the limpet Lottia gigantea. Proteome Sci. 2012;10:28–46.

69. Illies MR, Peeler MT, Dechtiaruk AM, Ettensohn CA. Identification and developmental expression of new biomineralization proteins in the sea urchin Strongylocentrotus purpuratus. Dev Genes Evol. 2002;212(9):419–31.

70. Tomanek RJ, Christensen LP, Simons M, Murakami M, Zheng W, Schatteman GC. Embryonic coronary vasculogenesis and angiogenesis are regulated by interactions between multiple FGFs and VEGF and are influenced by mesenchymal stem cells. Dev Dyn. 2010;239(12):3182–91.

71. Oulion S, Bertrand S, Escriva H. Evolution of the FGF Gene Family. Int J Evol Biol. 2012;2012:1–12.

72. Ornitz DM, Itoh N. The Fibroblast Growth Factor signaling pathway. Wiley Interdiscip Rev Dev Biol. 2015;4(3):215–66.

73. Itoh N, Ornitz DM. Evolution of the Fgf and Fgfr gene families. Trends Genet. 2004;20(11):563–9.

74. Morino Y, Koga H, Tachibana K, Shoguchi E, Kiyomoto M, Wada H. Heterochronic activation of VEGF signaling and the evolution of the skeleton in echinoderm pluteus larvae. Evol Dev. 2012;14(5):428–36.

75. Gao F, Thompson JR, Petsios E, Erkenbrack E, Moats RA, Bottjer DJ, et al. Juvenile skeletogenesis in anciently diverged sea urchin clades. Dev Biol. 2015;400(1):148–58.

76. Gao F, Davidson EH. Transfer of a large gene regulatory apparatus to a new developmental address in echinoid evolution. Proc Natl Acad Sci U S A. 2008 Apr 22;105(16):6091–6.

77. Materna SC, Howard-Ashby M, Gray RF, Davidson EH. The C2H2 zinc finger genes of Strongylocentrotus purpuratus and their expression in embryonic development. Dev Biol. 2006;300:108–20.

78. Kaneto S, Wada H. Regeneration of amphioxus oral cirri and its skeletal rods: implications for the origin of the vertebrate skeleton. J Exp Zool Part B Mol Dev Evol. 2011;316B(6):409–417.

79. Ferretti P, Health C. Regeneration of vertebrate appendages. eLS. 2013;1–7.

80. Ferguson C, Alpern E, Miclau T, Helms JA. Does adult fracture repair recapitulate embryonic skeletal formation? Mech Dev. 1999;87(1–2):57–66.

81. Okazaki K. Spicule formation by isolated micromeres of the sea urchin embryo. Integr Comp Biol. 1975;15(3):567–81.

82. Yang Y. Skeletal morphogenesis and embryonic development. In: Primer on the Metabolic Bone Diseases and Disorders of Mineral Metabolism. 2013. p. 1–14.

83. Koga H, Fujitani H, Morino Y, Miyamoto N, Tsuchimoto J, Shibata TF, et al. Experimental Approach Reveals the Role of alx1 in the Evolution of the Echinoderm Larval Skeleton. PLoS One. 2016;11(2):e0149067.

84. Koga H, Matsubara M, Fujitani H, Miyamoto N, Komatsu M, Kiyomoto M, et al. Functional evolution of Ets in echinoderms with focus on the evolution of echinoderm larval skeletons. Dev Genes Evol. 2010 Sep;220(3–4):107–15.

85. Rizzo F, Fernandez-Serra M, Squarzoni P, Archimandritis A, Arnone MI. Identification and developmental expression of the ets gene family in the sea urchin (Strongylocentrotus purpuratus). Dev Biol. 2006;300(1):35–48.

86. Zhao Q, Behringer RR, de Crombrugghe B. Prenatal folic acid treatment suppresses acrania and meroanencephaly in mice mutant for Cart1 homeobox gene. Nat Genet. 1996;13(3):275–83.

87. Li V, Raouf A, Kitching R, Seth A. Ets2 transcription factor inhibits mineralization and affects target gene expression during osteoblast maturation. In Vivo (Brooklyn). 2004;18(5):517–24.

88. Raouf A, Seth A. Ets transcription factors and targets in osteogenesis. Oncogene. 2000;19(55):6455–63.

89. Vlaeminck-Guillem V, Carrere S, Dewitte F, Stehelin D, Desbiens X, Duterque-Coquillaud M. The Ets family member Erg gene is expressed in mesodermal tissues and neural crests at fundamental steps during mouse embryogenesis. Mech Dev. 2000;91(1–2):331–5.

90. Kola I, Brookes S, Green AR, Garber R, Tymms M, Papas TS, et al. The Ets1 transcription factor is widely expressed during murine embryo development and is associated with mesodermal cells involved in morphogenetic processes such as organ formation. Proc Natl Acad Sci U S A. 1993;90(August):7588–92.

91. Iwamoto M, Tamamura Y, Koyama E, Komori T, Takeshita N, Williams JA, et al. Transcription factor ERG and joint and articular cartilage formation during mouse limb and spine skeletogenesis. Dev Biol. 2007;305(1):40–51.

92. Raouf A, Seth A. Discovery of osteoblast-associated genes using cDNA microarrays. Bone. 2002;30(3):463–71.

93. Jandzik D, Hawkins MB, Cattell M V, Cerny R, Square T a, Medeiros DM. Roles for FGF in lamprey pharyngeal pouch formation and skeletogenesis highlight ancestral functions in the vertebrate head. Development. 2014;141(3):629–38.

94. Mina M, Havens B. FGF signaling in mandibular skeletogenesis. Orthod Craniofacial Res. 2007;10:59=66.

95. Yu K, Ornitz DM. FGF signaling regulates mesenchymal differentiation and skeletal patterning along the limb bud proximodistal axis. Development. 2008;135:483–91.

96. Sarkar S, Petiot A, Copp A, Ferretti P, Thorogood P. FGF2 promotes skeletogenic differentiation of cranial neural crest cells. Development. 2001;128(11):2143–52.

97. Luo Y-J, Takeuchi T, Koyanagi R, Yamada L, Kanda M, Khalturina M, et al. The Lingula genome provides insights into brachiopod evolution and the origin of phosphate biomineralization. Nat Commun. 2015;6:1–10.

98. Jackson D, McDougall C, Green K, Simpson F, Worheide G, Degnan B. A rapidly evolving secretome builds and patterns a sea shell. BMC Biol. 2006;4(1):40.

99. Jackson DJ, McDougall C, Woodcroft B, Moase P, Rose RA, Kube M, et al. Parallel Evolution of Nacre Building Gene Sets in Molluscs. Mol Biol Evol. 2010;27(3):591–608.

100. Murdock DJE, Donoghue PCJ. Evolutionary origins of animal skeletal biomineralization. Cells Tissues Organs. 2011;194(2–4):98–102.

101. Dupont S, Thorndyke W, Thorndyke MC, Burke RD. Neural development of the brittlestar Amphiura filiformis. Dev Genes Evol. 2009 Mar;219(3):159–66.

102. Dupont S, Thorndyke MC. Growth or differentiation? Adaptive regeneration in the brittlestar Amphiura filiformis. J Exp Biol. 2006;209:3873–81.

103. Altenhoff AM, Glover NM, Train CM, Kaleb K, Warwick Vesztrocy A, Dylus D, et al. The OMA orthology database in 2018: Retrieving evolutionary relationships among all domains of life through richer web and programmatic interfaces. Nucleic Acids Res. 2018;46(D1):D477–85.

104. Katoh K, Rozewicki J, Yamada KD. MAFFT online service: multiple sequence alignment, interactive sequence choice and visualization. Brief Bioinform. 2017;(June):1–7.
105. Gouveia-Oliveira R, Sackett PW, Pedersen AG. MaxAlign: Maximizing usable data in an alignment. BMC Bioinformatics. 2007;8:1–8.
106. Nguyen LT, Schmidt HA, Von Haeseler A, Minh BQ. IQ-TREE: A fast and effective stochastic algorithm for estimating maximum-likelihood phylogenies. Mol Biol Evol. 2015;32(1):268–74.
107. Geiss GK, Bumgarner RE, Birditt B, Dahl T, Dowidar N, Dunaway DL, et al. Direct multiplexed measurement of gene expression with color-coded probe pairs. Nat Biotechnol. 2008;26(3):317–25.
108. Tinevez J-Y, Perry N, Schindelin J, Hoopes GM, Reynolds GD, Laplantine E, et al. TrackMate: an open and extensible platform for single-particle tracking. Methods. 2016;

Figures

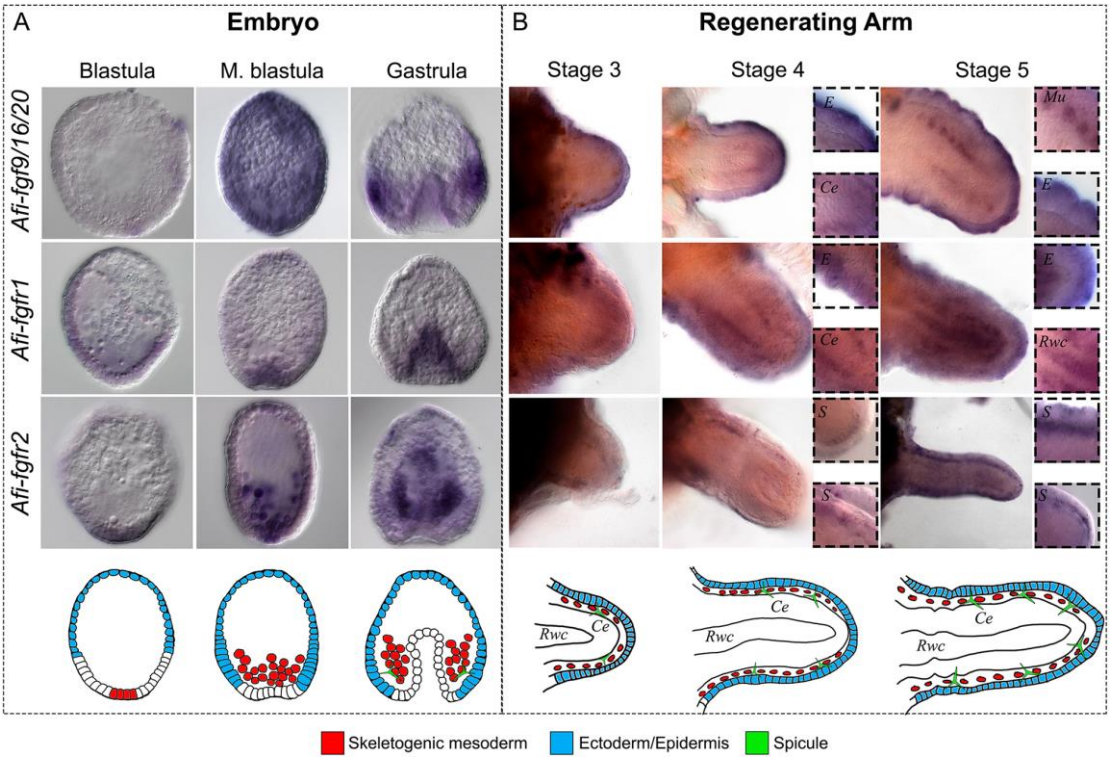

Figure 1: Expression of FGF signalling components in embryos and early regenerating arm stages of *A. filiformis*. A) Top: WMISH on embryos at blastula, mesenchyme blastula and gastrula stages of development showing expression of *Afi-fgf9/16/20, Afi-fgfr1, Afi-fgfr2*. Bottom: schematic diagram of major relevant cellular domains in corresponding stage embryos. B) Top: WMISH on regenerates at stages 3, 4 and 5 showing the expression of *Afi-fgf9/16/20, Afi-fgfr1, Afi-fgfr2.* Insets show detail of expression patterns. Bottom: Schematic diagram of major relevant cellular domains at corresponding stages. E – epidermis, Ce – coelomic epithelium, Mu – metameric units, Rwc - radial water canal, S – skeletogenic cells in dermal layer. Images from the aboral view. Scale bars: 100µm.

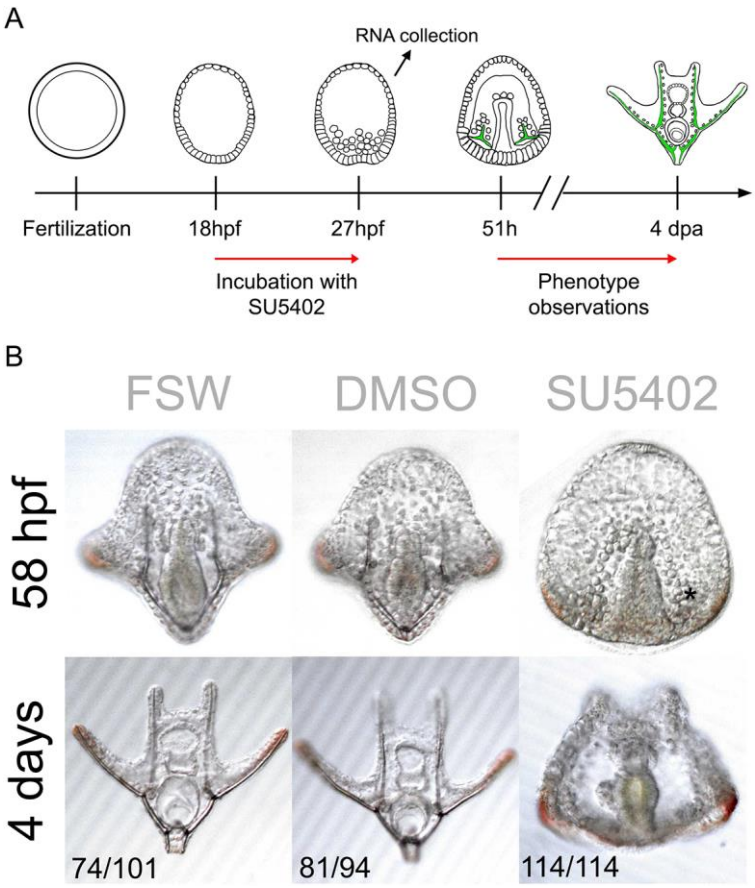

Figure 2: FGF signalling perturbation using the SU5402 inhibitor in brittle star embryos. A) Experimental procedure for SU5402 treatment. B) Phenotypic analysis of SU5402-treated *A. filiformis* embryos and controls at 58hpf and 4 days post-fertilization shows that perturbation of FGF signalling results in embryos with no skeletal spicules forming. Numbers at the bottom show counts for embryos observed with the represented phenotype/total embryos counted.

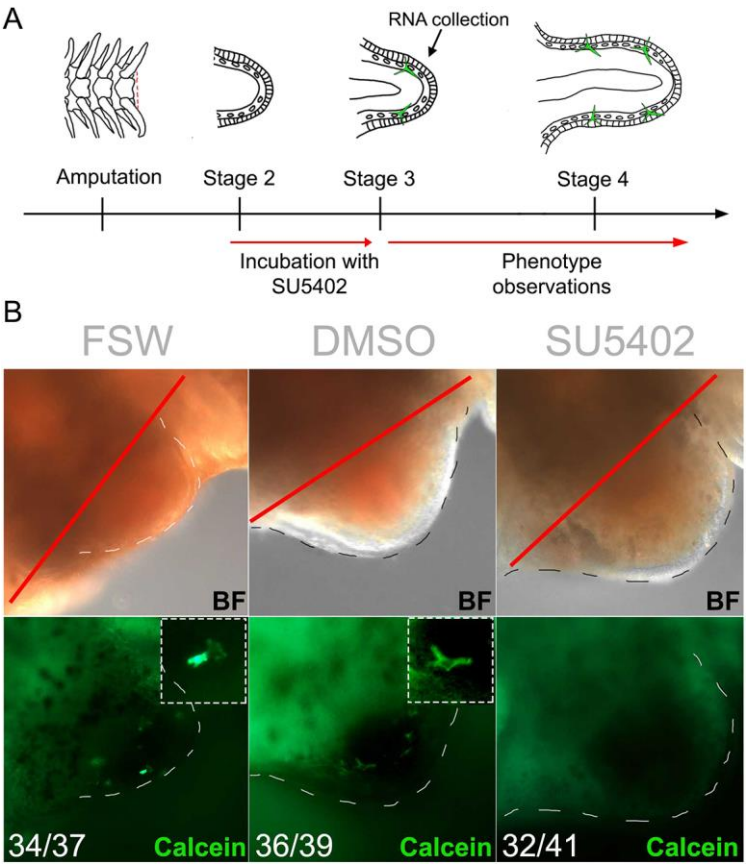

Figure 3: FGF signalling perturbation using SU5402 in brittle star regenerating arm explants. A) Experimental procedure for SU5402 treatment. B) Phenotypic analysis of SU5402-treated *A. filiformis* regenerates and controls at 24 hours post treatment (stage 3) shows that perturbation of FGF signalling inhibits spicule formation. Numbers at the bottom show counts for explants observed with the represented phenotype/total explants counted. Red line –amputation plane. Dashed lines – outline of regenerating bud.

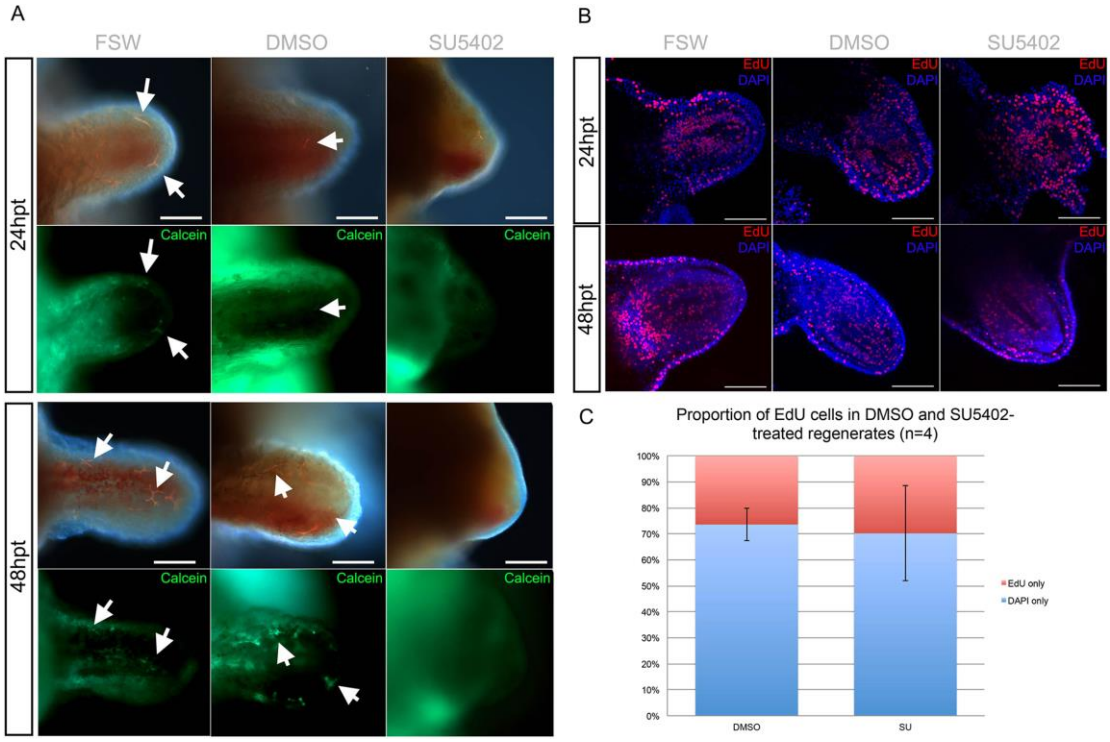

Figure 4: FGF signalling perturbation interferes with arm regeneration in *A. filiformis* but not by reducing cell proliferation. A) Phenotypic analysis of regenerating arm explants in control and SU5402 conditions at 24 hours post treatment (hpt) and 48hpt shows that skeletogenic spicules do not form and the arm seizes to regenerate further. Newly formed skeletal spicules are labelled by calcein in green. B) Confocal images of an EdU cell proliferation assay on control and treated regenerates shows no changes in the proportion of EdU labelled nuclei in SU5402-treated explants both at 24hpt and 48hpt. C) Quantification of the results in B showing no significant decrease in the proportion of EdU-labelled nuclei relative to all nuclei counted.

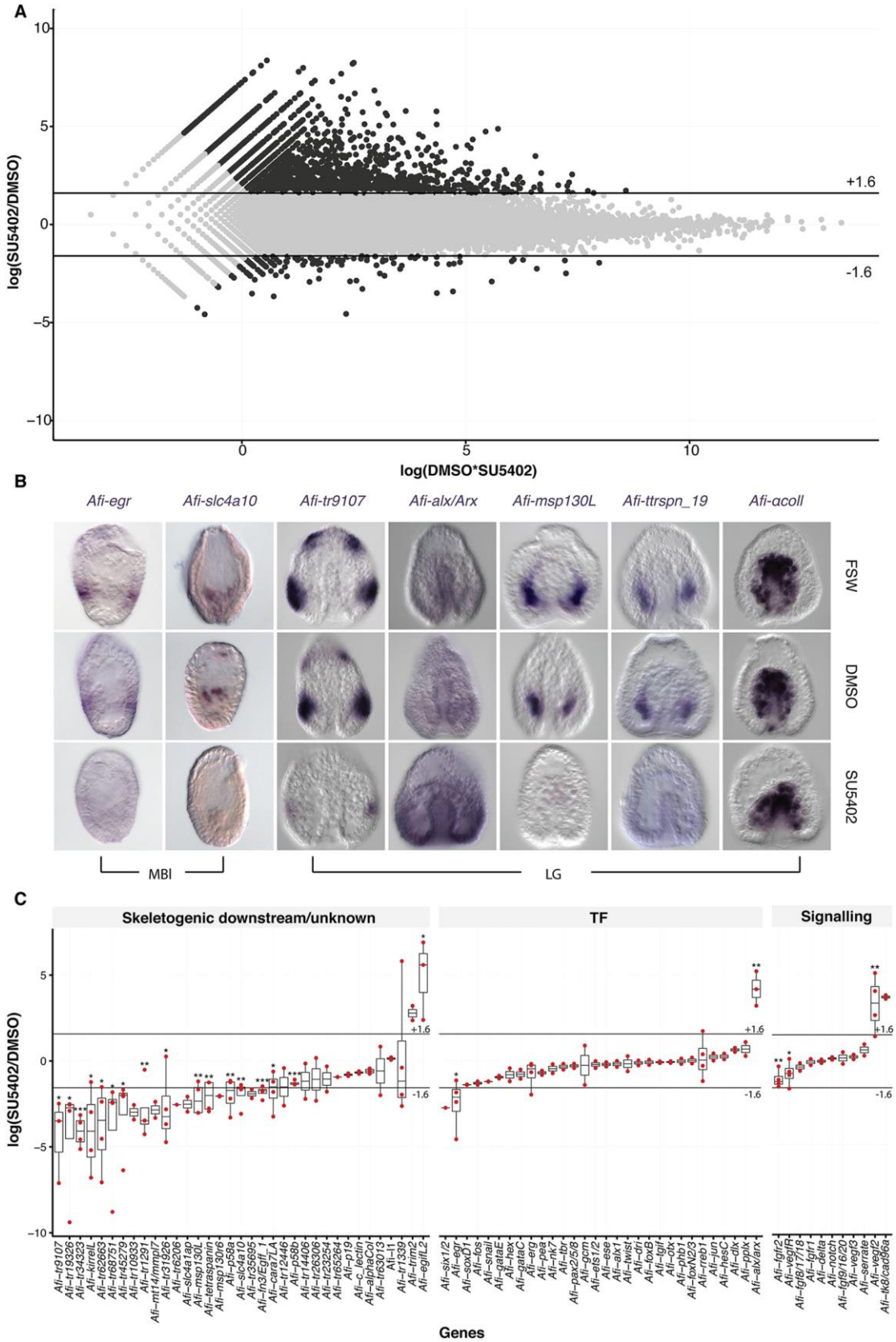

Figure 5: Differential transcriptomic analysis and WMISH for SU5402-treated and control embryos. (A) MA-plot showing upregulated genes in response to SU5402 treatment on top and downregulated genes on the bottom. (B) WMISH on embryos treated with SU5402 that were fixed at gastrula stage. *Afi-αcoll* was used as negative control and no change in expression is observed. *Afi-ttrspn 19, Afi-msp130L,* and *Afi-tr9107* are downregulated and *Afi-alx/arx* is upregulated in SU5402-treated samples. Embryos are all oriented with apical pole at the top and vegetal pole at the bottom. C) Box plot summarizing differential gene expression in SU5402-treated embryos relative to DMSO showing consistency between transcriptome, qPCR and NanoString quantification strategies represented as log2(SU5402/DMSO).

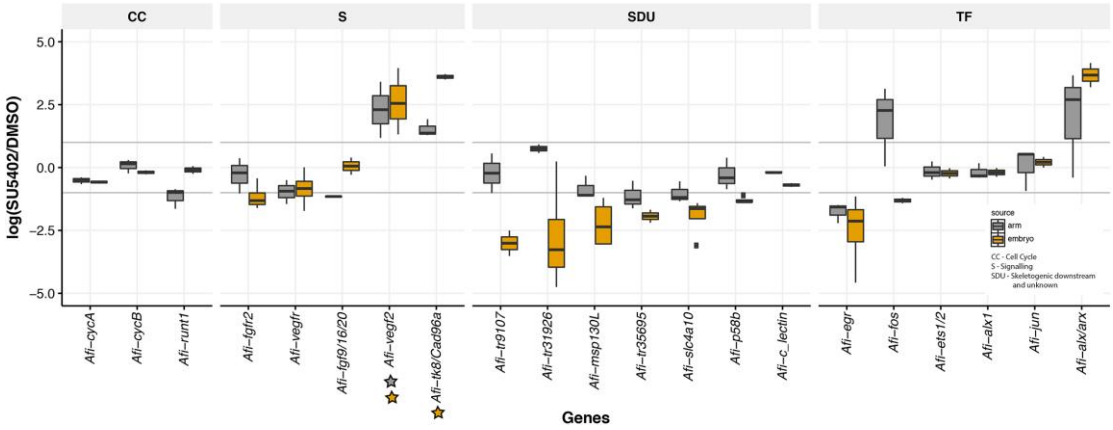

Figure 6: Comparison of genes affected by FGF signalling perturbation in embryos and regenerating arms of *A. filiformis*. Boxplot of selected genes showing the median and data distribution of gene quantification obtained in SU5402-treated embryos (grey) and regenerates (yellow) relative to DMSO controls, from at least 3 biological replicas. The relative abundance is expressed in log2(SU5402/DMSO) and threshold is set at ±1 corresponding to 2-folds of difference (gray horizontal line). Genes have been divided in functional categories: CC – cell cycle; S – signalling; SDU – skeletogenic downstream and unknown; TF – transcription factors. Stars under a gene indicate very low level of expression in control embryos (yellow – see Table S2) or in regenerating arms (grey – see Table S3).

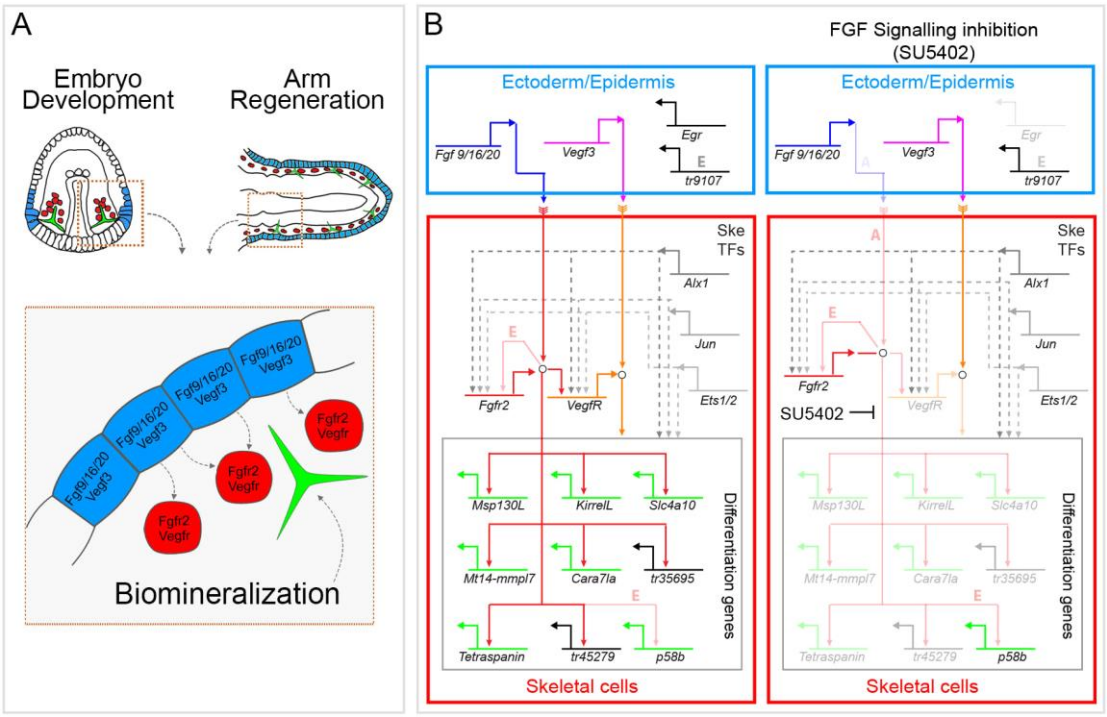

Figure 7: Role of FGF signalling in skeletal cells in embryos and adult regenerating arms of *A. filiformis*. A) Skeletal cellular arrangement in a gastrula embryo and a stage 3/4 regenerating arm when biomineralized skeleton is deposited. In both cases mesenchymal cells (red) adjacent to ectodermal/epidermal cells (blue) secrete in the extracellular space the biomineralized skeleton (green). The cartoon represents the signalling occurring from ectodermal/epidermal to mesenchymal cells. B) Left: hypothetical gene regulatory network for skeletal cells built with data coming from this work and previous publications (33–36). Genes are colour-coded and are represented by their cis-regulatory control system: green are orthologs of genes know to be essential in the biomineralization process in sea urchin; genes of unknown function but known expression domain are in black. Genes are connected by functional linkages, which are either inferred (dashed lines) or confirmed (solid lines) in this study. Arrows indicate positive inputs (activation) and barred line negative inputs (repression). Open circle

represent post-transcriptional/biochemical interactions occurring in the cytoplasm (phosphorylation of the FGF and VEGF receptors upon binding to the ligand and the complex intracellular cascade of signalling events). Right: represent the same network in presence of FGF signaling inhibitor (SU5402). Downregulated genes are shown in shaded colors. E are linkages present only in developing embryos and A only in regenerating arms.

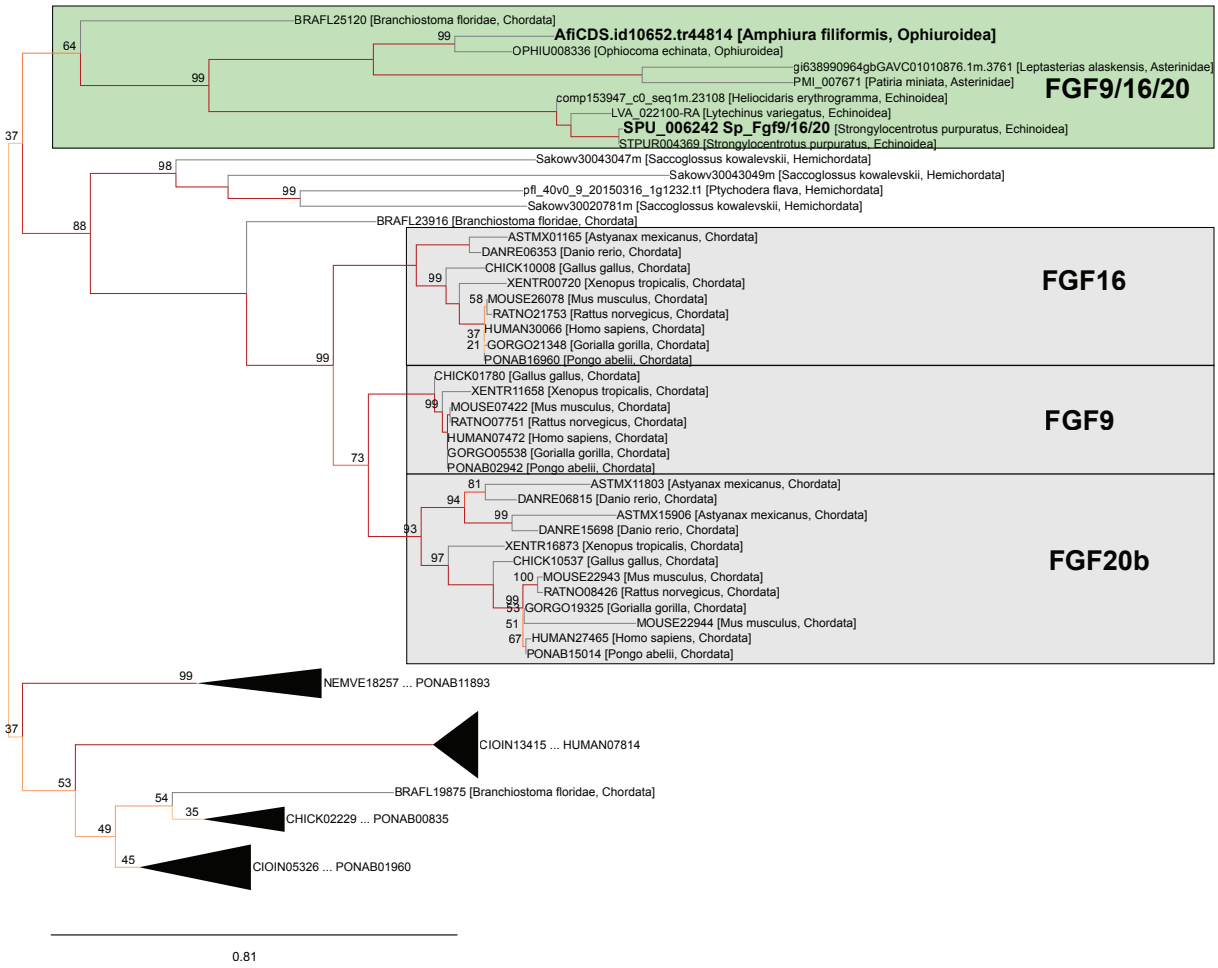

Figure S1: Tree for FGF9/16/20 genes. Maximum likelihood (ML) tree inferred using Iqtree (v.1.5.5) with LG model and 1000 fast bootstraps (1) with sequences derived from OMA group of FGF9/16/20 compute on 41 species (2,3). *Afi-fgf9/16/20,* along with other echinoderm FGF sequences, forms a well-supported group with the sea urchin *Sp-fgf9/16/20* gene (bootstrap 99), therefore considered an orthologous. The echinoderm *fgf9/16/20* genes form group related to vertebrate *FGF9*, *FGF16* and *FGF20* genes. On nodes are fast bootstrap values (1).

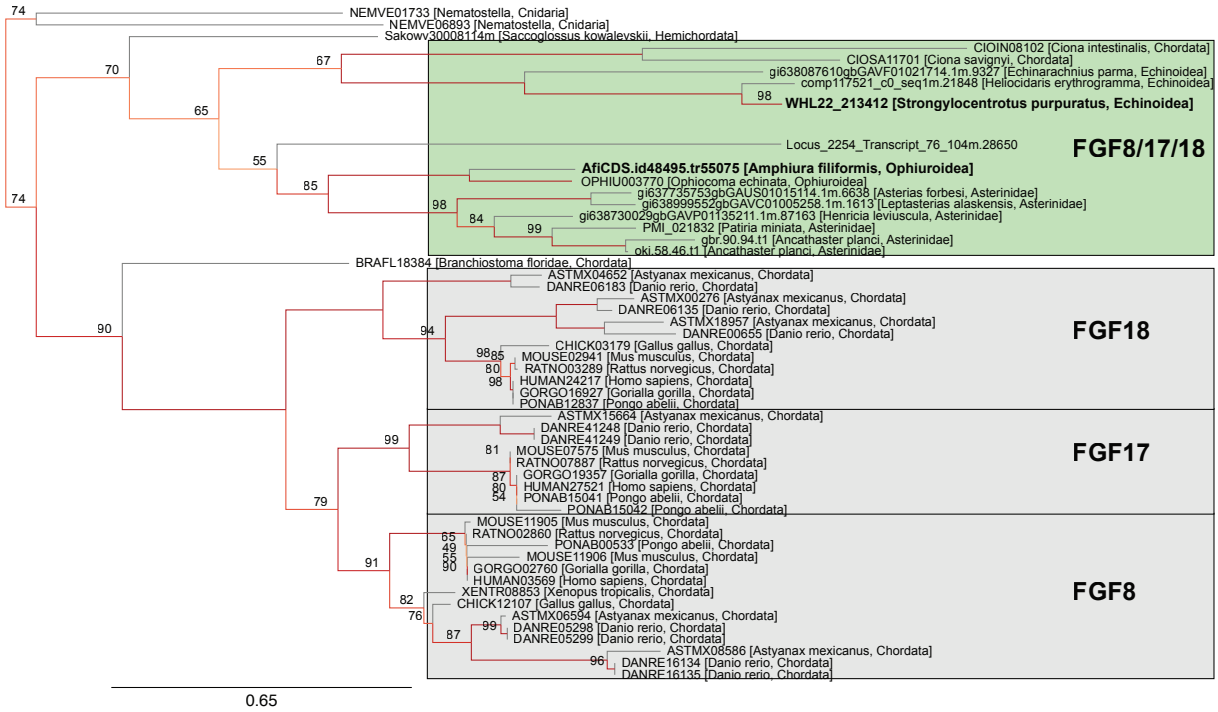

Figure S2: Gene tree for FGF8/17/18 ligands. ML Tree inferred with sequences derived from OMA group of FGF8/17/18 compute on 41 species (1, 2, 3). *Afi-fgf8/17/18* forms a group with a sea urchin sequence identified in the *S. purpuratus* transcriptome and the *S. kowalevskii fgf8/17/18* gene (bootstrap 70;(3)). This group has a clear relation to the group of chordate *FGF8*, *FGF17* and *FGF18* genes. On nodes are fast bootstrap values (1).

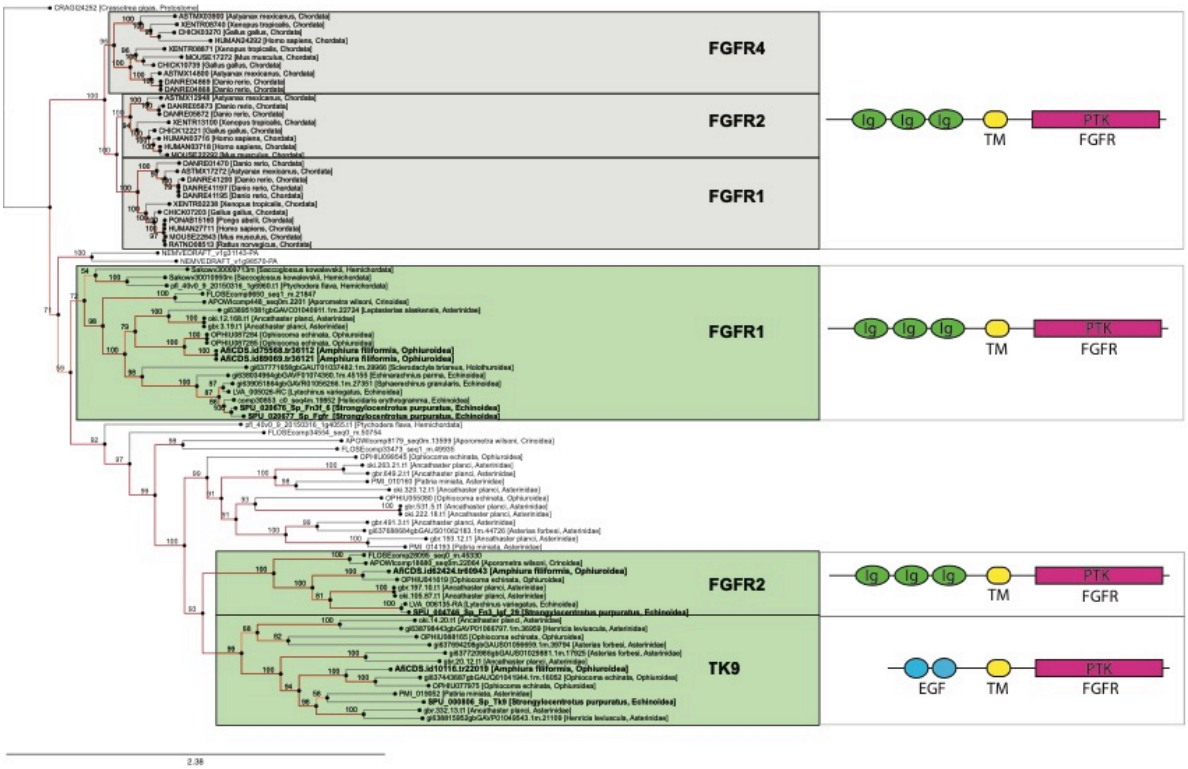

Figure S3: Gene tree for FGF receptors. ML tree inferred with sequences derived from OMA group of FGF receptors compute on 41 species (1, 2, 3). Three protein tyrosine kinase (PTK) sequences of the FGF receptor type have been identified in the *A. filiformis* transcriptome and here analysed along sea urchin, echinoderms and vertebrates sequences. *Afi-fgfr1*, *Afi-fgfr2* and *Afi-tk9* form well-supported groups with the *S. purpuratus* respective sequences (bootstrap of 99 and 100), therefore are considered orthologs to the sea urchin genes. All the echinoderms PTK in the tree are weakly related to the group of vertebrates FGFR 2, FGFR4 and FGFR1. The tree topology suggests independent duplication in echinoderms and in vertebrates of *fgfr* genes from a common gene in metazoans. On the right are schematically reported the protein conserved domain analyses that show the presence of PTK and trans membrane domains (TM) in each of the *A. filiformis* sequence, however only *Afi-fgfr1*, *Afi-fgfr2* encode for the three immunoglobulin extracellular domains (Ig) necessary to bind FGF ligands. On the contrary, the *Afi-tk9* sequence encodes for two extracellular epidermal growth factor (EGF) domains typical of other classes of PTK receptors, therefore we consider the *Afi-tk9* not a FGF receptor. On nodes are fast bootstrap values (1).

Figure S4: Gene tree for VEGF ligands. ML Tree inferred with sequences derived from OMA group of VEGF ligands compute on 41 species (1, 2, 3). *Afi-vegf2* and *Afi-vegf3* form well-supported groups with the sea urchin and other echinoderms *vegf2* and *vegf3* (bootstrap 96 and 98 respectively) genes, we therefore consider them orthologs to their sea urchin counterparts. The tree suggests that both ligand genes are descendants from an ancestral *vegf* gene that got independently duplicated in chordates. On nodes are fast bootstrap values (1).

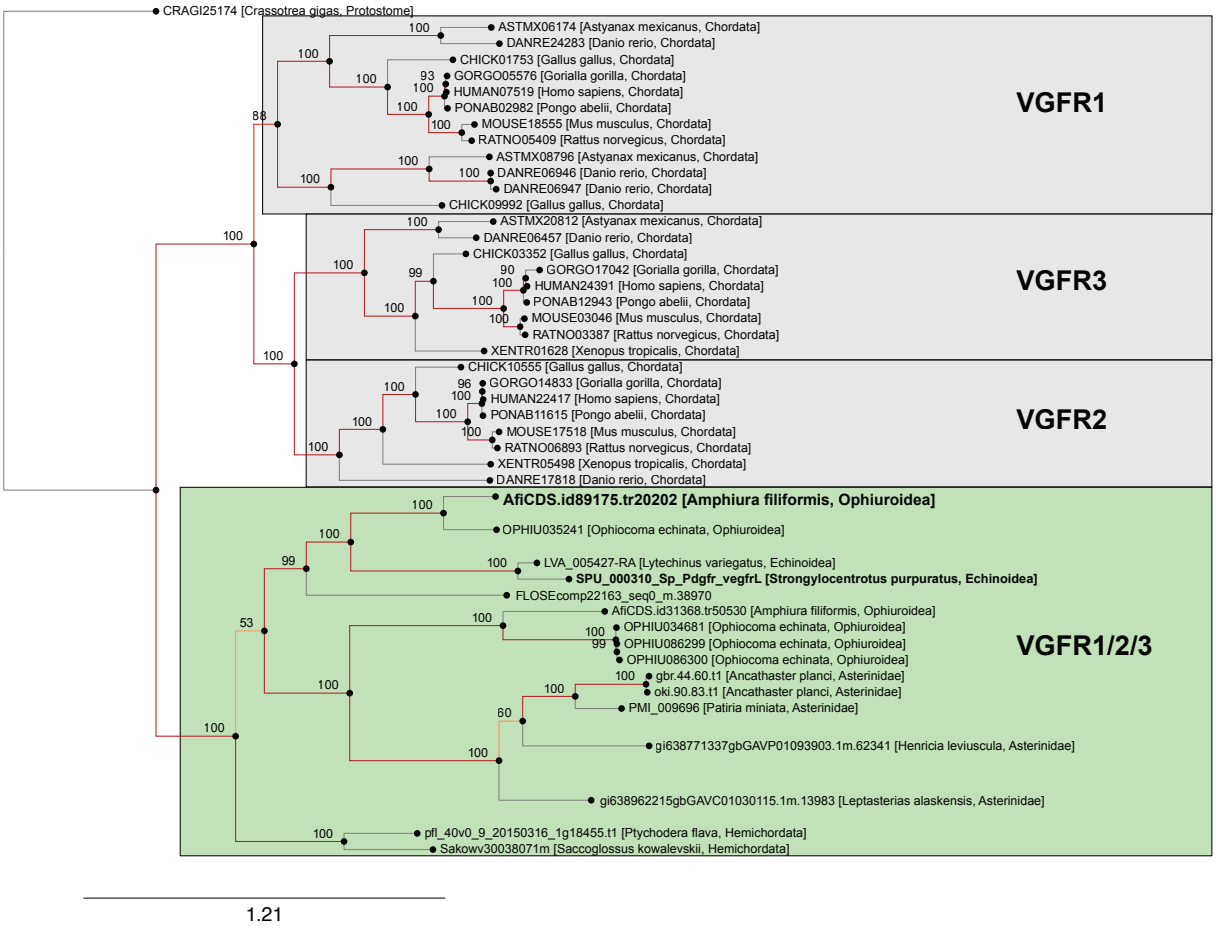

Figure S5: Gene tree for VEGF receptor. ML Tree inferred with sequences derived from OMA group of VEGF receptors compute on 41 species (1, 2, 3). A single Vegf receptor sequence has been identified in the *A. filiformis* transcriptome. *Afi-vegfr* groups to *S. purpuratus vegfr* gene (bootstrap 99) and is related to the chordate group of *Vegfr* genes (VEGFR1, VEGFR2 and VEGFR3). On nodes are fast bootstrap values (1).

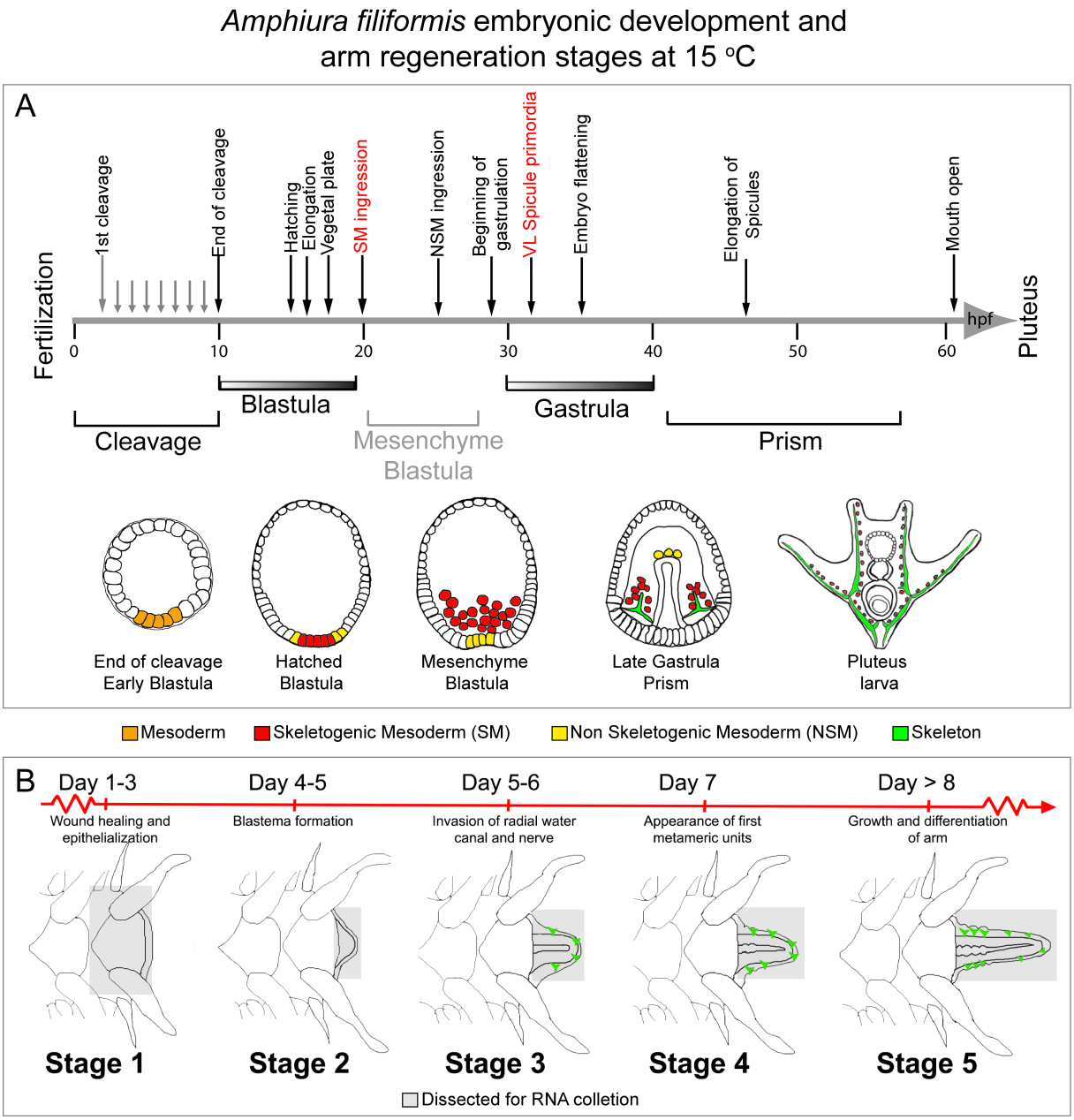

Figure S6: *A. filiformis* developmental and regeneration timeline. A) Embryonic timeline in hours post fertilization (hpf) with highlighted major event occurring, the specification of the skeletogenic mesodermal (SM) lineage and the formation of biomineralized skeleton(4). B) Timeline of major regenerative events and staging system expressed in days post amputation (dpa)(5). The wound healing, epithelialization and the absence of active cell proliferation characterize stage 1. At Stage 2 cell proliferation became very prominent and a small regenerative bud (or blastema) is visible. Stage 3 is characterized by a well-structured regenerative bud with clear regenerating radial water canal (RWC), radial nerve chord (RNC) and the appearance of skeleton primordia. Stage 4 shows the formation of the first metameric unit in most proximal position, while Stage 5 is considered when several metameric units are visible.

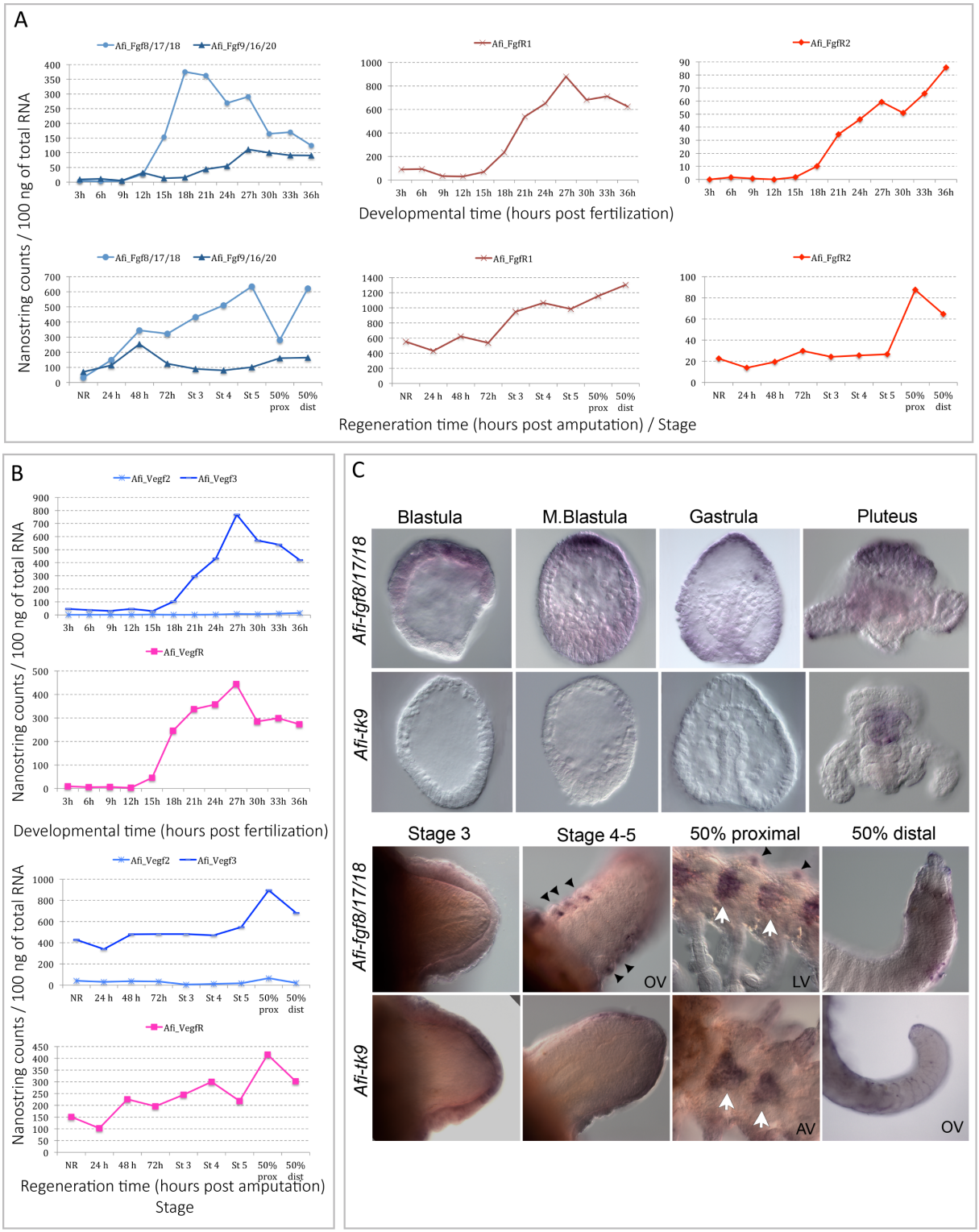

Figure S7: Expression profiles of FGF and VEGF signalling component genes during embryonic development and arm regeneration in *A. filiformis*. A) Levels of expression of *Afi-fgf9/16/20*, *Afi-fgf8/17/18*, *Afi-fgfr1* and *Afi-fgfr2* in embryos and adult non-regenerating and regenerating arms at different stages. B) Expression profiles of *Afi-vegf2*, *Afi-vegf3*, and *Afi-vegfr* in embryos and adult non-regenerating and regenerating arms at different stages. Transcript abundance is represented as

NanoString counts per 100ng of Total RNA. Hpf – hours post fertilization, hpa – hours post amputation, prox – proximal, dist – distal, NR – non-regenerating. C) WMISH on *Afi-fgf8/17/18* and *Afi-tk9* at different embryonic developmental stages and in early and late stages of adult arm regeneration in *A. filiformis*. *Afi-fgf8/17/18* shows expression in the apical region of the ectoderm throughout all the embryonic stages analysed and in the apical organ of the pluteus larva. In the regenerates WMISH identifies specific expression in spines at stage 4/5 and in late regeneration also in the vertebras. *Afi-tk9* shows no expression during embryonic development. Specific staining is identified in the foregut of the larva. In the early regenerating stages and the distal tip of the late regenerates the probe for *Afi-tk9* stains specifically the epidermis, while in proximal elements the vertebras are also showing expression. White arrows – expression in vertebrae, Black arrowheads – expression in spines. LV – lateral view, AV – aboral view, OV – oral view. Embryos are all oriented with apical pole at the top and vegetal pole at the bottom; regenerating arms are oriented with proximal on the left and distal on the right.

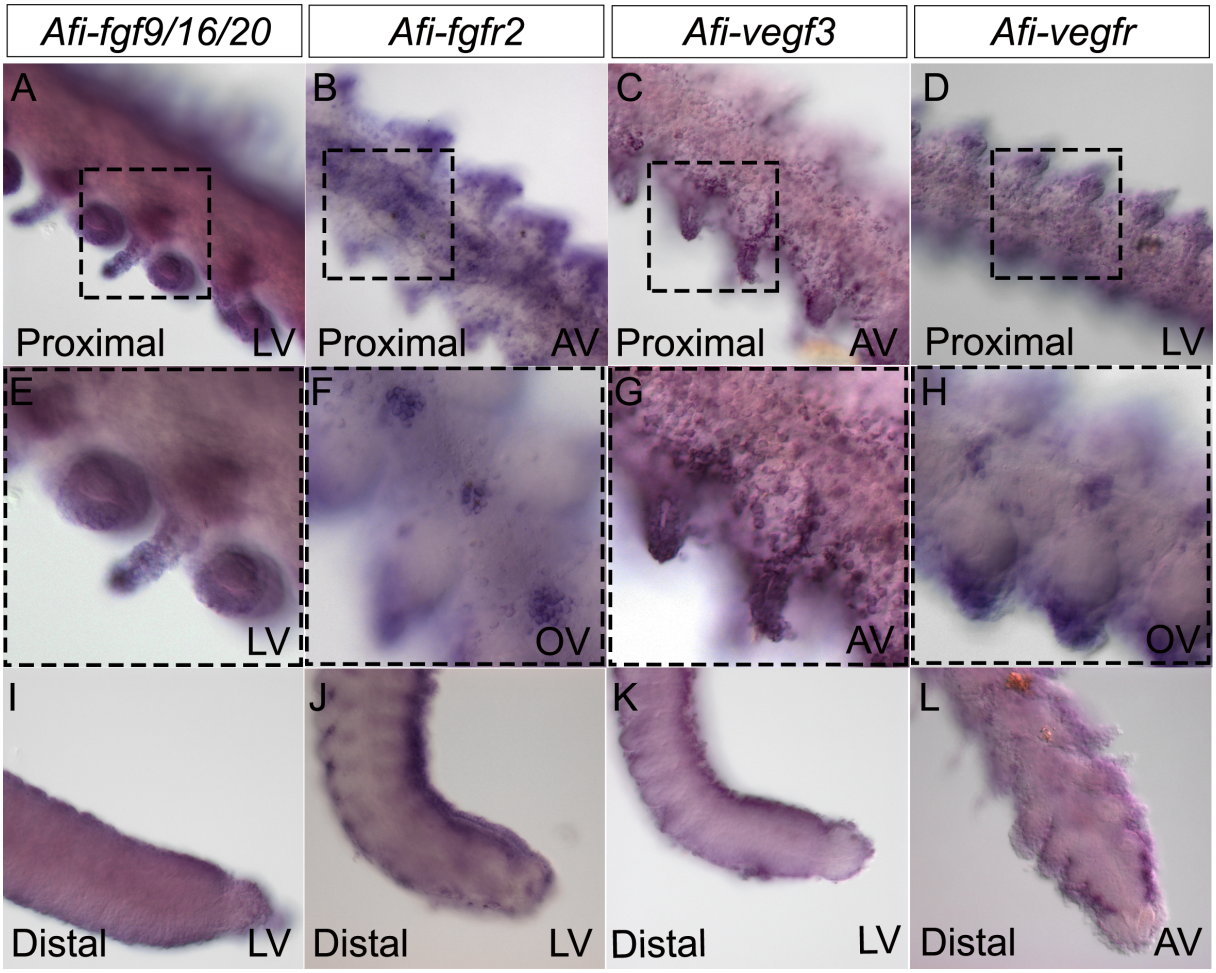

Figure S8: Expression of FGF and VEGF genes at late stages of arm regeneration in *A. filiformis*. WMISH conducted in 50% regenerative arms reveal: *Afi-fgf9/16/20* (A, E and I) still expressed in the epidermis both of proximal and distal structures. *Afi-fgfr2* (B,F and J) probe detects the developing skeletal elements such as vertebras and lateral shields in the proximal, most developed, part of the regenerates, while in the distal tip the staining is confined to the dermal cells. Similarly, the *Afi-vegf3* (C, G and K) is detected epidermal structured throughout the late regenerate, while the *Afi-vegfr* is revealed in developing skeletal elements and dermal cells. Av – aboral view, OV – oral view, LV – lateral view. Regenerating arms are oriented with proximal on the left and distal on the right.

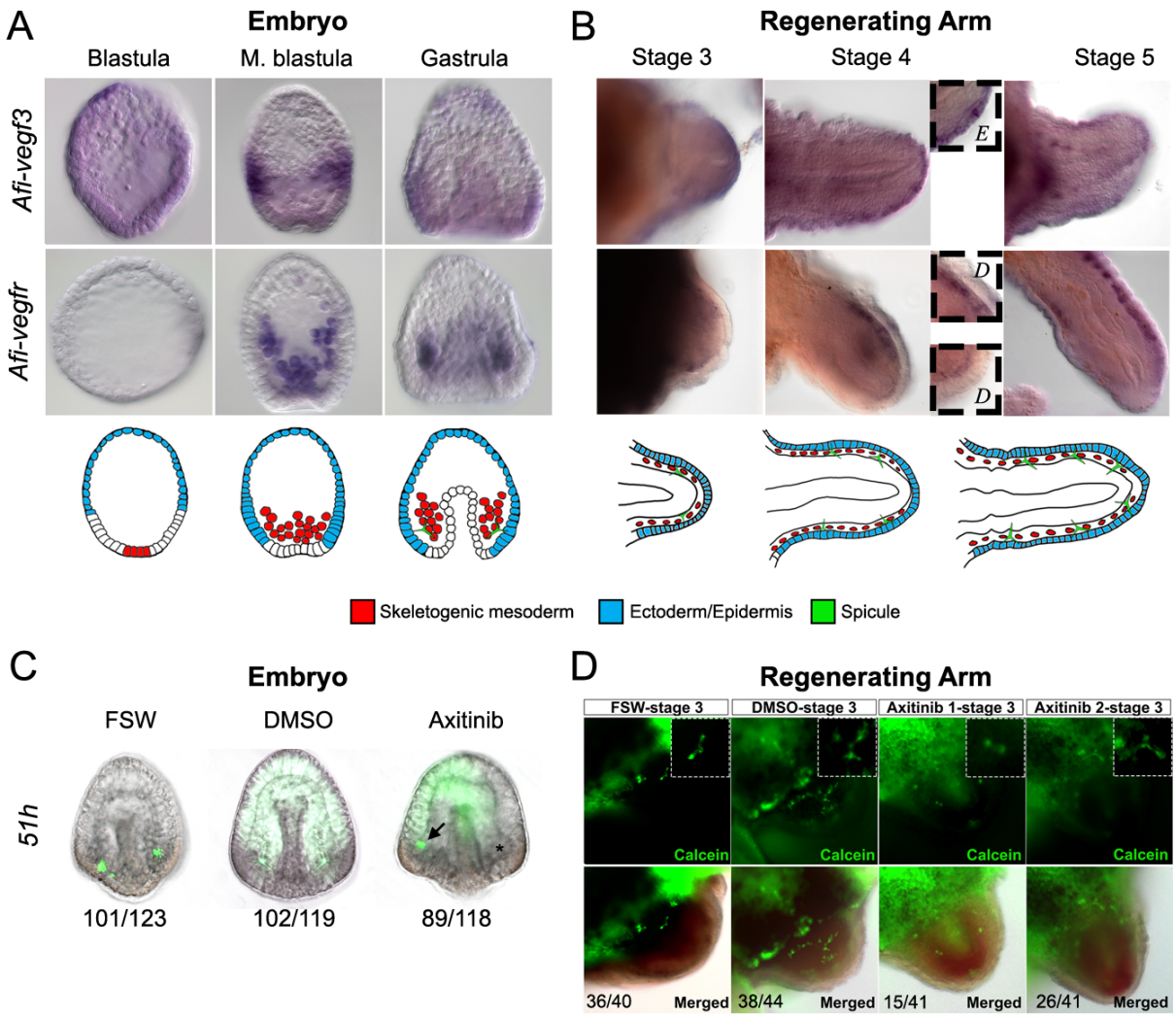

Figure S9: Expression of VEGF signalling components and axitinib treatment in embryos and early regenerating arm stages of *A. filiformis*. A) Top: WMISH on embryos at blastula, mesenchyme blastula and gastrula stages of development showing the expression of *Afi-vegf3* and *Afi-vegfr*. Bottom: schematic diagram of major relevant cellular domains. B) Top: WMISH on regenerates at stages 3, 4 and 5 showing the expression of *Afi-vegf3* and *Afi-vegfr*. Insets show detail of expression patterns. Bottom: Schematic diagram of major relevant cellular domains in regenerates. C) Phenotypic analysis of axitinib-treated embryos (75 nM) and controls at 51 hpf shows that perturbation of VEGF signalling results in embryos with one skeletal spicule forming. Numbers at the bottom show counts for embryos observed with the represented phenotype/total embryos counted. D) Phenotypic analysis of axitinib-treated regenerates and controls at 24 hours post treatment (stage 3) show that perturbation of VEGF signalling either results in normal or slightly reduced skeletal spicules. Numbers at the bottom show counts for explants observed with the represented phenotype/total explants counted. Insets show magnification of skeletal phenotypes. Embryos are all oriented with apical pole at the top and vegetal pole at the bottom; regenerating arms are oriented with proximal on the left and distal on the right.

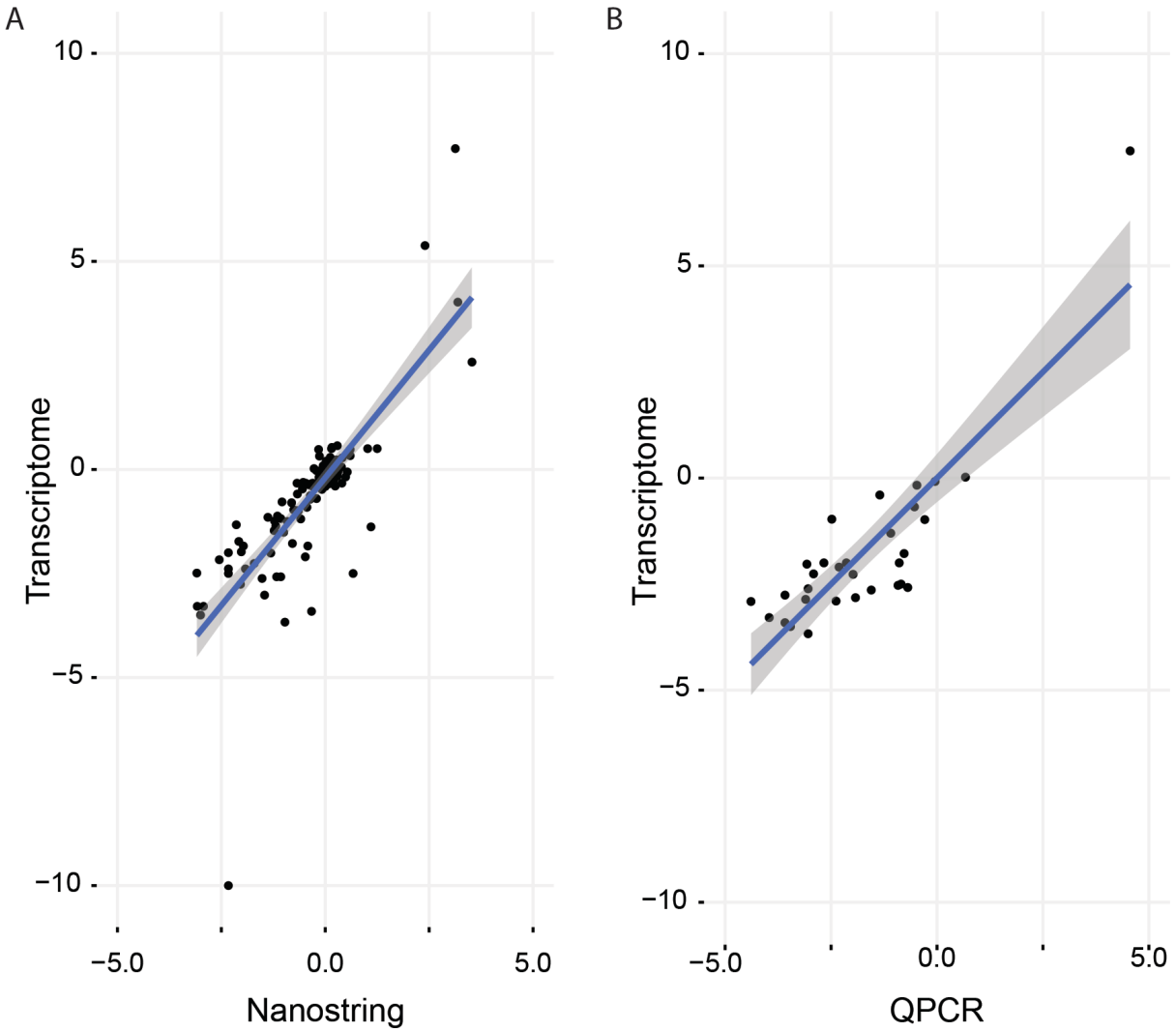

Fig S10: Comparison of differential expression values obtained from quantitative data collected on the same sample using all three technologies (RNA-seq, QPCR and NanoString). Linear regression was used to identify conversion factors as means to bring all data from different biological replicates on a comparable quantitative scale (Transcriptome). A) Comparison between Transcriptome and NanoString quantification strategies in embryos of *A. filiformis*. A significant linear regression was found ($F(1,111)= 292.3$, p-value: < 2.2e-16), with an $R2$ of 0.7247. B) Comparison of Transcriptome and QPCR quantification strategies in same embryo RNA samples of *A. filiformis*. A significant linear regression was found ($F(1,29)= 78.25$, p-value: <9.877e-10), with an $R2$ of 0.7203. Details are available in Methods.

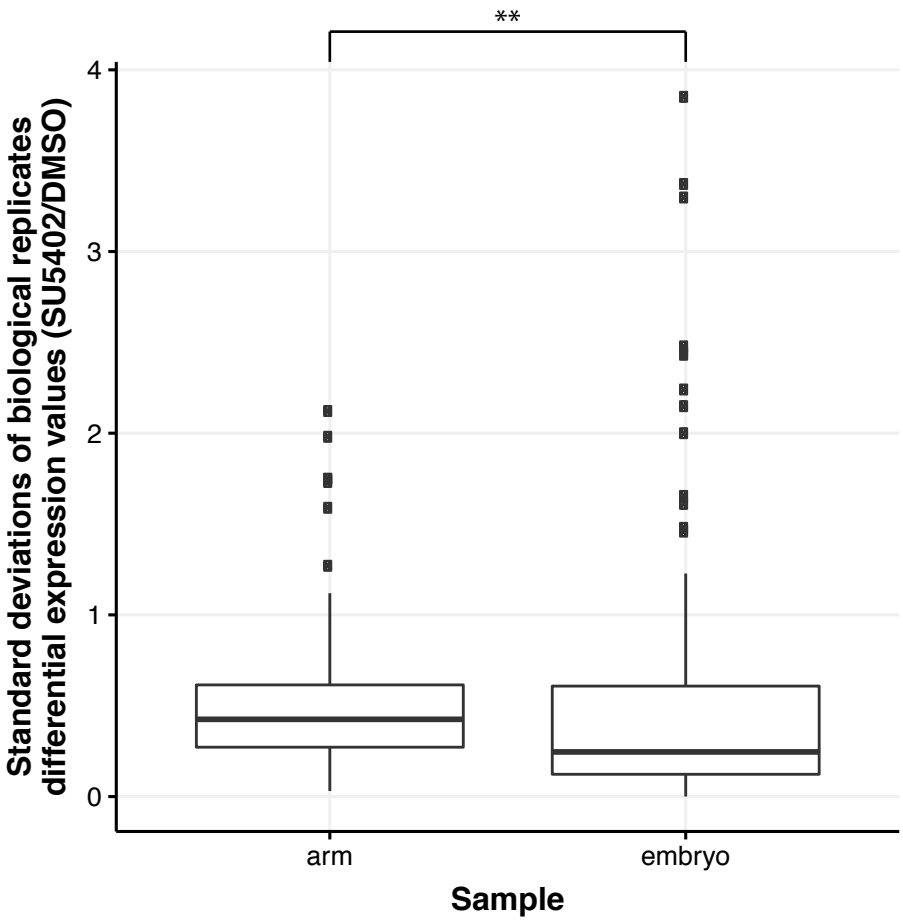

Figure S11: Standard deviations of differential expression are significantly lower in embryos than in arms. Boxplot was obtained using standard deviation values taken from at least 3 biological replicates for arm and embryo respectively as presented in Fig S12. A higher median in arm indicates that individual replicates in arms are displaying a higher dispersion than in embryos. This difference is significant (Wilcox-rank test p-value=0.002329).

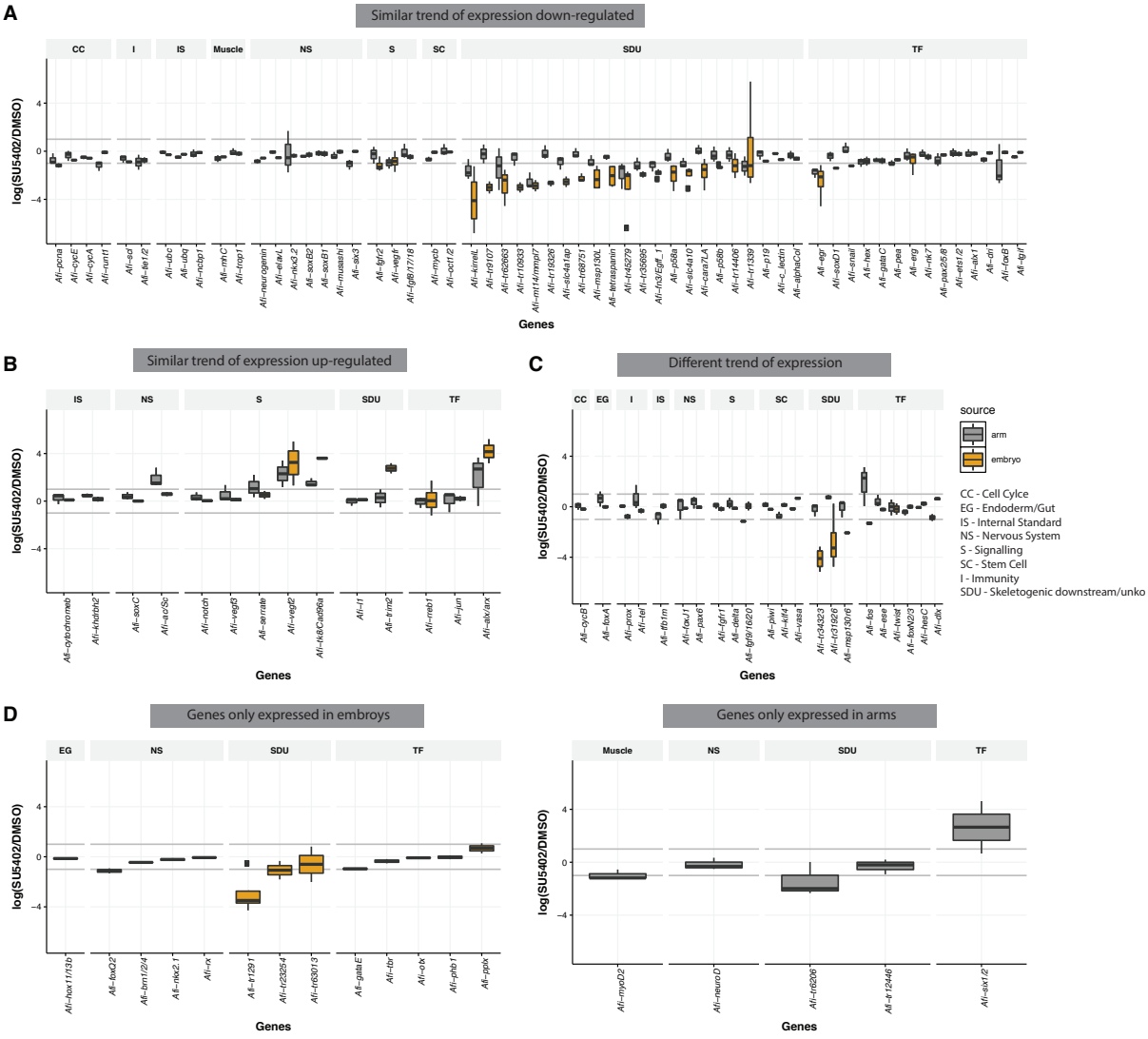

Figure S12: Comparison of genes affected by SU5402 treatment in embryos and regenerating arms of the brittle star. Boxplot showing the median and data distribution of at least 3 biological replicates across different technologies (analysed as described in methods) of gene quantification in SU5402 treated embryos (grey) and regenerates (yellow) relative to DMSO controls. A) Downregulated genes that show similar trends between embryos and regenerates; B) similar trends in upregulated genes. C) Genes that have opposite trend in expression between embryos and regenerates. In D) are genes expressed above background levels exclusively during embryonic development; and E) only during regeneration. The relative abundance is expressed in log2(SU5402/DMSO) and threshold is set at ±1 log2(SU5402/DMSO) corresponding to 2-folds of difference (grey horizontal line). Genes downregulated in the SU5402 treatment have negative values and genes upregulated positive. Genes have been divided in functional categories: CC – cell cycle; EG – endoderm/gut; IS – internal standard; NS – nervous system; S – signalling; SC – stem cells; I – immunity; SDU – skeletogenic downstream/unknown; TF – transcription factors.

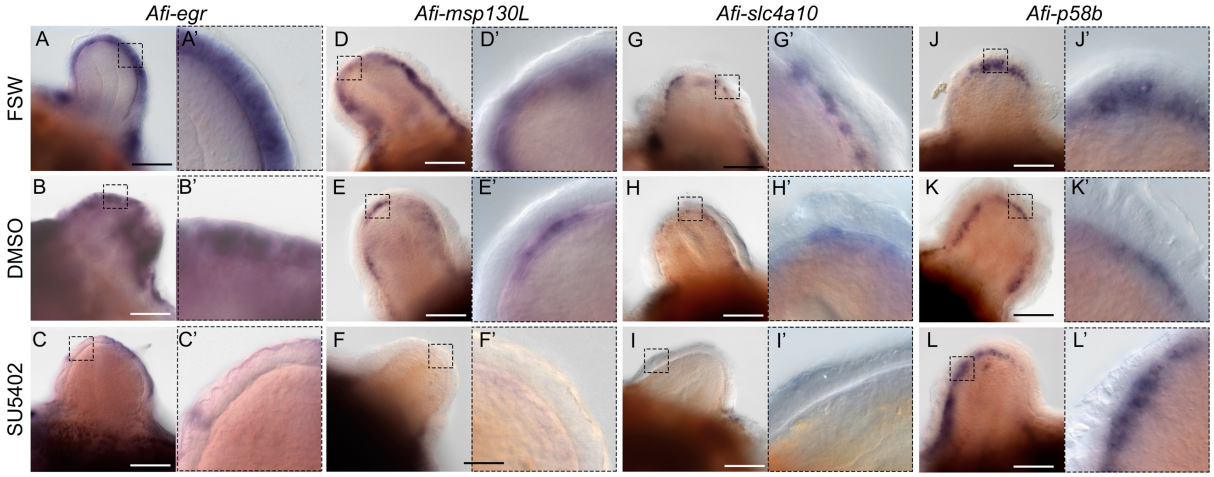

Figure S13: Spatial downregulation of selected genes in regenerating arm samples treated with SU5402 compared to controls. A-C) WMISH on regenerating arms shows normal expression of *Afi-egr* in epidermis is downregulated in SU5402-treated samples. A'-C') Same images at higher magnification. D-F) WMISH on regenerating arms shows normal expression of *Afi-msp130L* in the skeletogenic dermal layer is downregulated in SU5402-treated samples. D'-F') Same images at higher magnification. G-I) WMISH on regenerating arms shows normal expression of *Afi-slc4a10* in the skeletogenic dermal layer is downregulated in SU5402-treated samples. G'-I') Same images at higher magnification. J-L) WMISH on regenerating arms shows normal expression of control gene *Afi-p58b* in the skeletogenic dermal layer is maintained SU5402-treated samples. J'-L') Same images at higher magnification. Scale bars: 100μm.

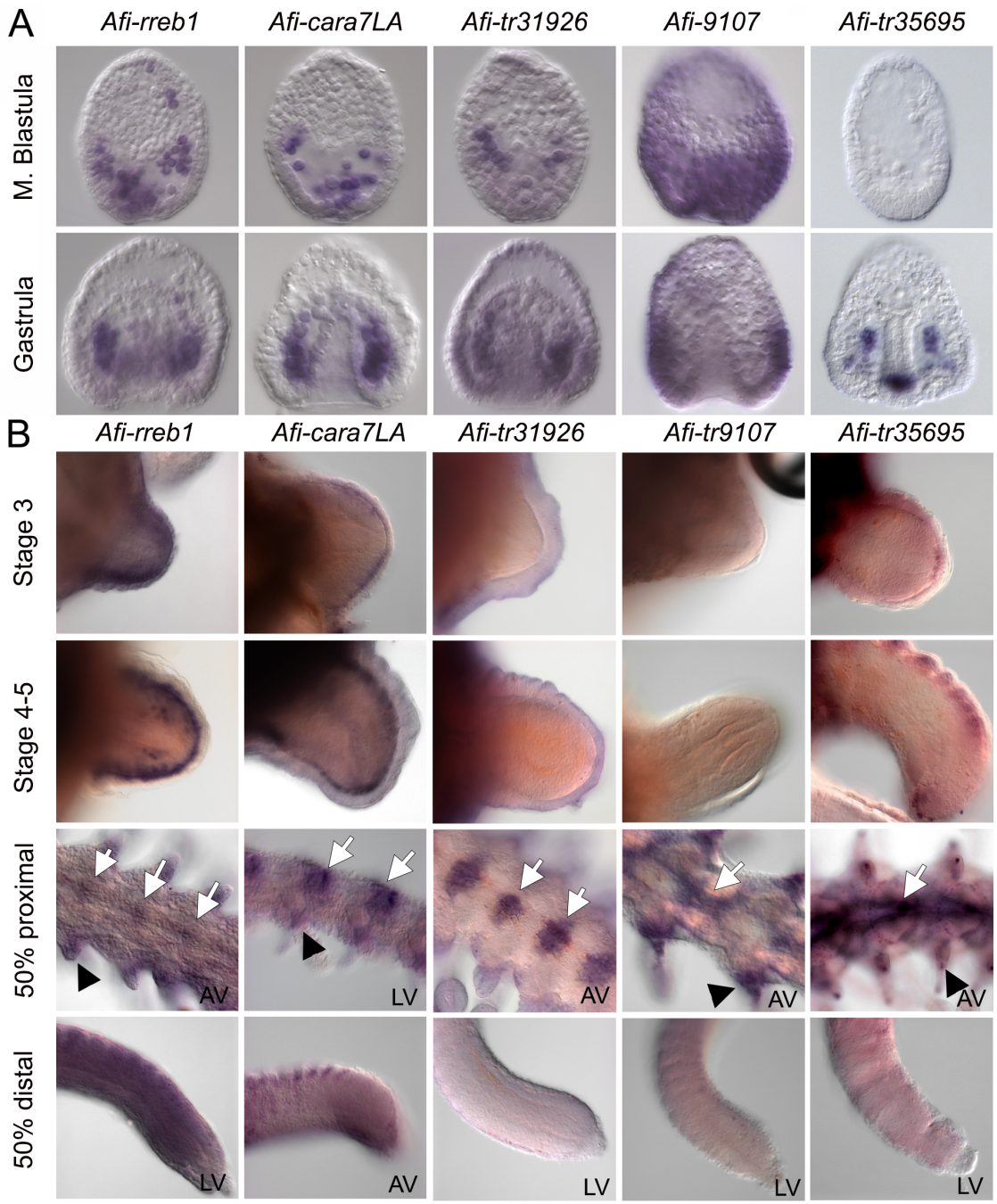

Figure S14: Novel identified genes are expressed in skeleton forming cells. WMISH on five genes: *Afi-rreb1, Afi-cara7La, Afi-tr31926, Afi-tr9107,* and *Afi-tr35695* at (A) mesenchyme blastula and gastrula stages of embryogenesis and (B) early and late stages of adult arm regeneration in the brittle star. All genes are expressed in skeletal cells sometime in development and regeneration. Exception is *Afi-tr9107* that shows expression in the ectoderm in a domain similar to the two ligands *fgf9/16/20* and *vegf3.* White arrows – expression in vertebrae, Black arrowheads – expression in spines. LV – lateral view, AV – aboral view. Embryos are all oriented with apical pole at the top and vegetal pole at the bottom; regenerating arms are oriented with proximal on the left and distal on the right.

Movie 1: Control and SU5402-treated regenerating arm explants are alive and motile after 48h of treatment.

Table S1

Click here to download Table S1

Table S2

Click here to download Table S2

Table S3

Click here to download Table S3

Table S4

Click here to download Table S4

Table S5

Click here to download Table S5

Table S6

Click here to download Table S6

Table S7

Click here to download Table S7

Supplementary references:

1. Nguyen LT, Schmidt HA, Von Haeseler A, Minh BQ. IQ-TREE: A fast and effective stochastic algorithm for estimating maximum-likelihood phylogenies. Mol Biol Evol. 2015;32(1):268–74.
2. Altenhoff AM, Levy J, Zarowiecki M, Vesztrocy AW, Dalquen DA, Müller S, et al. OMA standalone : orthology inference among public and custom genomes and transcriptomes. Genome Reseach. 2019;29:1–12.
3. Altenhoff AM, Glover NM, Train CM, Kaleb K, Warwick Vesztrocy A, Dylus D, et al. The OMA orthology database in 2018: Retrieving evolutionary relationships among all domains of life through richer web and programmatic interfaces. Nucleic Acids Res. 2018;46(D1):D477–85.
4. Dylus DV, Czarkwiani A, Stångberg J, Ortega-Martinez O, Dupont S, Oliveri P. Large-scale gene expression study in the ophiuroid Amphiura filiformis provides insights into evolution of gene regulatory networks. Evodevo. 2016;7(1).
5. Czarkwiani A, Ferrario C, Dylus D V., Sugni M, Oliveri P. Skeletal regeneration in the brittle star Amphiura filiformis. Front Zool. 2016;13:18.